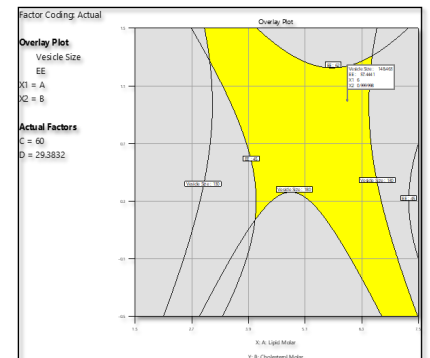
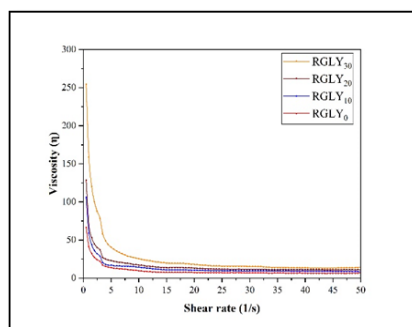
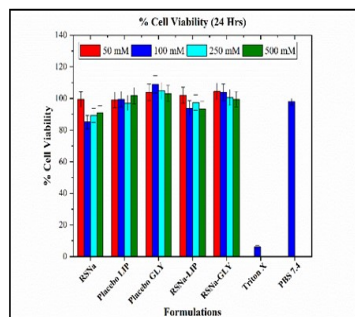


# Chapter-6

## Formulation development of RSNa loaded glycerosomes



**Stability study**



**Evaluation of RSNa loaded glycerosomes**

### 6.1. Selection of method for preparation of glycosomes:

This present work includes trial of 2 methods for formulation development of risedronate loaded glycosomes.

#### 1. Lipidic thin film hydration method:

Lipid S-75 and cholesterol were dissolved in organic solvent mixture of chloroform and methanol (1:1 v/v) in 50 mL round bottom flask. Then organic solvent was evaporated by rotary evaporator under reduced vacuum at  $60\pm 5^{\circ}\text{C}$  for 30 minutes at 150 rpm to form uniform thin layer of lipid phase. The traces of organic solvent were removed by keeping film in desiccator under reduced pressure for overnight. Risedronate was dissolved into glycerol aqueous solution and the prepared dried thin film was then hydrated with this solution (5 mL) at  $50^{\circ}\text{C}$  for 1 hr at 150 rpm. The obtained dispersion was sonicated with 60 % amplitude (2 sec ON and 2 sec OFF; 20 cycles). Then dispersion was purified by passing through sephadex G-25 column to remove untrapped drug. Then, the purified glycosomes were stored at  $2-8^{\circ}\text{C}$  for further study [1, 2].

#### 2. Reverse phase solvent evaporation method:

Lipid S-75 and cholesterol were dissolved in methanol: chloroform (in ratio of 1:1), while aqueous phase containing risedronate and glycerol was dissolved in double distilled water. The aqueous phase was added to the organic phase at a ratio of 1:3 (v/v) and sonicated for 30 min in a bath sonicator to form a uniform dispersion. The organic solvents were then removed by rota evaporator to obtain a dry film. The resulting prepared film was hydrated with glycerol aqueous solution and sonicated in an ice water bath on probe sonicator with 60 % amplitude (2 sec ON and 2 sec OFF; 20 cycles). Then dispersion was purified by passing through sephadex G-25 column to remove untrapped drug. Then, the purified glycosomes were stored at  $2-8^{\circ}\text{C}$  for further study [3].

The selection of suitable method for preparation of glycosomes was based on minimum vesicle size (VS) and maximum entrapment efficiency (%EE).

## **6.2. Selection of lipids:**

By keeping other formulation and process variables constant, different lipids and their combination were tried. Lipoid S-75, Lipoid S-100, DPPC, Phospholipon 90H, DSPC and Phospholipon 80H were used for screening of lipids. The lipid was selected on the basis of maximum entrapment efficiency and minimum vesicle size.

## **6.3. Drug-Excipients interaction studies by FTIR:**

The interaction between pure drug (RSNa) and mixture of excipients (lipid and cholesterol) was analysed by FTIR (Bruker, Germany). Thin KBr pellet was prepared and data were collected in the range of 400 to 4000  $\text{cm}^{-1}$  to determine compatibility of excipients with drug. (Mentioned in chapter no. 4 – Preformulation study, Section 4.2 and 4.4)

## **6.4. Identification of independent variables and qualitative risk assessment using Ishikawa diagram**

All possible variables which were linked with the development of RSNa loaded glycosomes were represented with the help of Ishikawa diagram. These factors were considered as 'low, moderate and high risk' based on their predicted effect on VS and % EE.

## **6.5. Optimization:**

After selection of method of preparation (Lipidic thin film hydration method) and lipid (Lipoid S-75), to identify the process and formulation variables which could significantly affect the vesicle size and % entrapment efficiency. The various variables for preliminary include speed of rotation for film hydration and film formation, solvent evaporation time, hydration time, hydration volume, hydration medium, lipid:drug molar ratio, cholesterol:drug molar ratio, amplitude of sonication, sonication cycles and glycerol concentration. Amongst these, the lipid:drug molar ratio, cholesterol:drug molar ratio, amplitude of sonication and sonication cycles found to be more critical variables which showed significant effect on vesicle size and entrapment efficiency. Hence, these were optimized by definitive screening method (surface response methodology).

### 6.6. Screening and optimization of process variables:

Following process variables were optimized by one factor at a time (OFAT) approach based on minimum VS and maximum % EE (shown in table- 6.1.).

Table- 6.1. Process variables studied for glycosomes formulation development

Variables	Screened values/range	
<b>Amplitude of sonication</b>	10	70
<b>Sonication cycles</b>	10	35
<b>Sonication cycle time</b>	2 sec ON, OFF	5 sec ON, OFF

### 6.7. Screening and optimization of formulation variables:

Following formulation variables were optimized by one factor at a time (OFAT) approach based on maximum entrapment efficiency and minimum vesicle size (shown in table-6.2).

Table- 6.2. Formulation variables studied for glycosomes formulation development

Variables	Screened values/range	
<b>Lipid:drug molar ratio</b>	2:1	9:1
<b>Cholesterol:drug molar ratio</b>	0:1	1:1
<b>Glycerol concentration (%)</b>	5	40
<b>Hydration Medium</b>	Distilled water	PBS 7.4
<b>Hydration Volume (mL)</b>	5	10

### 6.8. Optimization of RSNa loaded glycosomes by Definitive Screening Design (DSD):

The four variables namely Lipid:drug molar ratio, Cholesterol:drug molar ratio, Amplitude and cycle of sonication were selected as independent factors which act as high-risk factors effects on the vesicle size and % EE of prepared glycosomes and optimized by Definitive Screening Design (DSD) using software DesignExpert@V13 (Stat-Ease, Inc., USA). Total 13 runs, four factors, three levels DSD design were used to studied the effect of

independent variables on dependent variables. The summary of independent and dependent variables with the goal set of response is shown in table-6.3.

Table- 6.3. Variables selected for DSD for optimization of RSNa loaded Glycosomes.

<b>Independent Variables</b>		
<b>Variables</b>	<b>Low Level</b>	<b>High Level</b>
<b>Lipid:drug molar ratio (A)</b>	3:1	6:1
<b>Cholesterol:drug molar ratio (B)</b>	0:1	1:1
<b>Amplitude (C)</b>	40	60
<b>Cycles of sonication (D)</b>	15	30
<b>Dependent Variables</b>		
<b>Variables</b>	<b>Goal</b>	<b>Importance</b>
<b>Vesicle Size (Y1)</b>	Minimize	+++
<b>% EE (Y2)</b>	Maximize	+++

### 6.9. Characterization of RSNa loaded glycosomes:

- a. The average vesicle size, polydispersity index (PDI) and zeta potential (surface charge) were analyzed by photon correlation spectroscopy using Malvern zetasizer Nano-ZS 90 (Malvern Instrument, Worcestershire, United Kingdom). All samples were analyzed in triplicate and analysis was performed after 24 hrs of their preparation [4].

The morphology of formulated vesicles was confirmed by transmission electron microscopy (TEM). Samples were placed on carbon coated copper grid, stained with phosphotungstic acid (1%) and allowed to stand for drying [1, 5].

The residual solvents study was performed by gas chromatography (Perkin Elmer, USA) to check that if they are present, rather present in permissible limits or not. The standard solution of chloroform and methanol was prepared in order to produce 10 ppm while sample was prepared in similar dilution order of standard for comparison. After obtaining the chromatogram of standard samples, formulation samples were analyzed and compared to reference sample of chloroform and methanol [6-8].

**b. % Entrapment Efficiency (% EE) and % Drug Loading Capacity (%DLC):**

The free RSNa was separated by using a sephadex G-25 column for the determination of entrapment efficiency. The RSNa loaded glycerosomal dispersion was passed through the Sephadex G-25 column followed by distilled water. Firstly, the vesicular dispersion was eluted from the column, and then the free drug was eluted. The fractions of both entrapped and free drug samples were collected in different eppendorf tubes. The collected samples were dissolved in methanol and analysed by a UV-visible spectrophotometer at 262 nm [9]. The % EE was calculated as follows:

$$\%EE = \frac{\text{Total RSNa} - \text{Free RSNa}}{\text{Total RSNa}} \times 100$$

.....equation- 6.1.

The % drug loading capacity (% DLC) was calculated as follows [10]:

$$\%DLC = \frac{\text{Amount of entrapped in RSNa in glycerosomes}}{\text{Total solid content}} \times 100$$

.....equation- 6.2.

**6.10. Effect of glycerol concentration on RSNa loaded glycerosomes:**

The effect of change in concentration of glycerol on physicochemical characteristics, *in vitro* drug release and *ex vivo* skin permeation were analyzed. The RSNa loaded glycerosomes were prepared by using optimized parameters obtained from design with change in concentration of glycerol at time of hydration. The different batches were prepared by varying glycerol concentration from 10 to 30% w/w and compared with liposomes. All-prepared batches were analysed for physicochemical characteristics, *in vitro* drug release and *ex vivo* skin permeation study. The glycerol concentration was optimized on the basis of *in vitro* drug release and higher permeation of drug through skin. The selected optimized batch was used for further analysis i.e., *in vitro* cell line study, *in vivo* pharmacokinetic and pharmacodynamic study.

**c. Deformability Index:**

Deformability index of glycosomes was measured by extrusion method. The vesicular dispersion was extruded through polycarbonate filters of pore size of 100 nm at constant pressure. The deformability index was calculated by following equation:

$$DI = J \left[ \frac{r_v}{r_p} \right]^2 \dots\dots\dots\text{equation- 6.3}$$

Where, J is fraction of dispersion collected after extrusion (it should be within 0 to 1, in which 0 represents no fraction recovered, while 1 represents 100% of the dispersion recovered),  $r_v$  is the size of vesicles following extrusion in nm, and  $r_p$  is the pore size of the extruder (nm) [2].

**6.11. *In vitro* drug release study:**

The *in vitro* drug release from RSNa solution and all RSNa loaded glycosomes (having glycerol concentration from 0 - 30% w/w) was performed to study effect of glycerol concentration on drug release rate from glycosomes. Drug solution and RSNa loaded glycosomes was diffused through dialysis bag having MW cut-off of 12k-14k Da. The dialysis was performed in 50 mL of saline phosphate buffer pH 7.4. The samples of each formulation were withdrawn from the receptor medium and replaced with freshly prepared receptor medium to maintained sink condition at predetermining time interval over 48 hrs [1]. The withdrawn samples were analyzed by HPLC method (described in chapter-3).

**6.12. *Ex vivo* skin permeation study:**

*Ex vivo* skin permeation study was performed using abdominal skin of health Sprague Dawley rat (weighing 200-250 gm) as a membrane. The rat skin was sandwiched between donor and receptor compartment, in which stratum corneum faced towards donor's compartment and dermal side of skin was allowed in contact to saline phosphate buffer pH 7.4 in receptor compartment. The *ex vivo* permeation studies were carried out on Franz diffusion cell having diffusion area of 5 cm<sup>2</sup>. The receptor compartment was filled with PBS 7.4 and kept at 32 ± 0.5°C under stirring. To study effect on skin permeation of drug solution and glycosomes of different concentration (0-30% w/w), drug solution

and formulations (equivalent to drug solution concentration) were applied on donor compartment. The amount of drug diffused through rat skin was determined by withdrawing samples at predetermined time interval for 48 hrs and replaced receptor media with same amount of freshly prepared PBS 7.4 to maintain sink condition [4]. The withdrawn samples were analyzed by HPLC method [11].

The skin was removed from Franz diffusion cell after study completion and the donor side was washed with PBS and collected the washed sample for calculation of drug remained on skin. The skin was then cut into small pieces and suspended into PBS. The suspension was homogenized for 15 min and sonicated using bath sonicator to remove drug which was accumulated into skin layers. After that, the samples were centrifuged for 10 minutes at 5000 rpm. The supernatant was collected and filtered through 0.45  $\mu\text{m}$  syringe filter and analyzed to estimate drug retained in the skin [12-15].

The data obtained were plotted as % cumulative drug permeated through skin as a function of time. The drug remained-on skin and retained on skin was calculated. The transdermal flux and permeation enhancement ratio was calculated [16].

### **6.13. *In vitro* cell line study:**

#### **Cell culture:**

Skin fibroblast cells were purchased from NCCS, Pune, India and grown in T-25 cell culture flask incubated in CO<sub>2</sub> incubator in 5% CO<sub>2</sub> and 100% humidity at 37°C. The culture growth media contain DMEM (high glucose), 10% of foetal bovine serum and 1% of antibiotic solution [17, 18].

#### **i) Cytotoxicity assessment by MTT assay:**

The skin fibroblast cells-3T3 (7500 cells/well) were seeded in 96-well plates filled with 200  $\mu\text{L}$  of culture growth medium. After 24 hrs, the cells were washed with sterile phosphate buffer 7.4 and replaced with fresh growth medium. Then cells were treated for 12 and 24 hrs with drug solution, placebo formulations and drug loaded formulations. Each sample was tested in triplicates. The cells treated with PBS 7.4 and Triton X 100 were used as positive and negative control respectively. The remaining procedure was same as described in chapter -5 [2, 4, 19].

**ii) *In vitro* cell permeability study:**

The procedure for *In vitro* cell permeability study was same as reported in chapter-5. The samples of pure drug and their formulations equivalent to 300 µg prepared in growth medium were placed on the AP side, and 2.5 mL of DMEM on the BL side. Samples (200 µL) were withdrawn from BL compartments at predetermined time interval over 12 hrs. Withdrawn samples were stored at – 20 °C until analyzed by HPLC (described in chapter - 3). The apparent permeability coefficient ( $P_{app}$  in cm/s) from apical-to-basolateral was calculated as follows:

$$P_{app} = \frac{\text{Flux}}{\text{Initial concentration}} \quad \dots\dots\dots\text{equation- 6.4.}$$

Where,  $P_{app}$  is the apparent permeability co-efficient (cm/s).

**6.14. Stability study:**

The storage stability of drug loaded liposomes and glycosomes was carried out in air tight container at different temperatures viz. 2-8°C, 25±2°C/60±5 % RH and 40±2°C/75±5 % RH for 90 days. Samples were monitored by analysing for average vesicles size and % assay at interval of 15 days [5, 20].

## **6.15. Results and discussion:**

### **RSNa loaded glycosomes: Formulation development**

The formulation and evaluation of RSNa-loaded glycosomes, as well as the determination of a variety of critical factors that influence vesicle size and % EE, are all included in the current study. The critical variables were identified and chosen, and they underwent preliminary study to determine their suitable working ranges. These ranges were then applied to optimize each of the variables applying surface response methods.

## **6.16. Preliminary screening for RSNa loaded glycosomes:**

### **6.16.1. Risk analysis and mitigation:**

Risk analysis is the identification of critical factors whose small variations can result in a deterioration in product quality. The FishBone diagram (Figure- 6.1) was created based on a literature analysis and preliminary study to identify formulation and process factors that might affect the quality of glycosomes formulation development. The quality goal or critical quality attributes (CQA) for RSNa-loaded glycosomes was improved entrapment efficiency and minimum vesicle size. From the preliminary screening, variables with a moderate or medium impact on the glycosomes were optimised using the One Variable At a Time (OVAT) approach, whereas high-risk components were considered and optimised using the DSD (table- 6.4). In this scenario, only process and formulation parameters were investigated for risk assessment, whereas drug substance attributes were believed to remain constant because the drug used was from the same lot number throughout the study.

Table- 6.4. Risk analysis to identify critical parameters for formulation of RSNa loaded glycosomes

Critical Quality Attributes (CQA)	Process variables		Formulation Variables		
	Amplitude of sonication	Sonication cycles	Lipid: drug molar ratio	Cholesterol: drug molar ratio	Glycerol concentration
Vesicle Size (d.nm)	H	H	H	H	M
Entrapment efficiency (%)	H	H	H	H	H

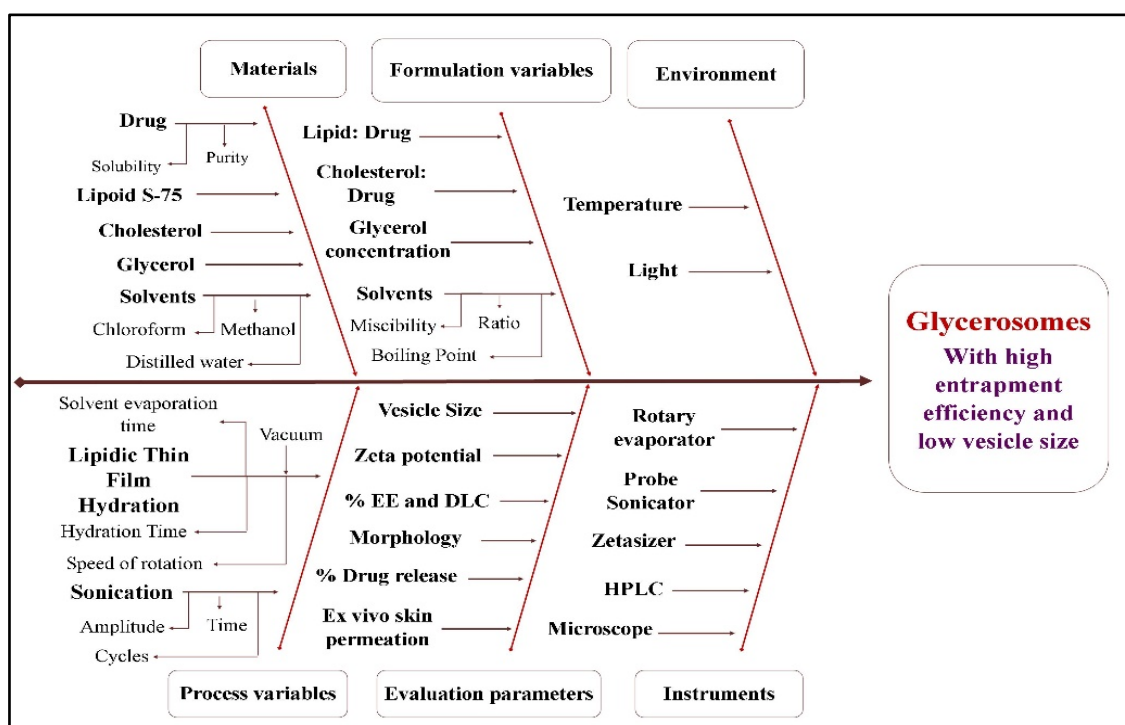


Figure- 6.1. FishBone diagram for selection of variables for development of glycosomes

### 6.16.2. Selection of method of preparation and lipid:

The choice of the most appropriate methodology is a key factor in the development of glycosomes. Vesicle size and entrapment efficiency were significantly influenced by technique selection in contrast to lipid selection. We tried the thin lipidic film hydration

and reverse phase evaporation methods, among the several reported methods. The thin lipidic film hydration approach was chosen for the preparation of glycosomes based on minimum vesicle size and maximum entrapment efficiency. Lipoid S-75 had the highest entrapment efficiency with the smallest vesicle size among the various lipids and their combinations (shown in table- 6.5). Therefore, Lipoid S-75 was chosen as the lipid for formulating glycosomes.

Table- 6.5. Selection of method of preparation and lipid

<b>Selection of method of glycosomes preparation</b>		
<b>Method of preparation</b>	<b>Observation</b>	
	<b>Vesicle Size (d.nm)</b>	<b>Entrapment efficiency (%)</b>
Lipidic thin film hydration method	208.8 ± 5.45	32.02 ± 0.93
Reverse phase evaporation method	352.6 ± 19.40	27.23 ± 1.06
<b>Selection of lipid</b>		
<b>Lipid and their combination</b>	<b>Observation</b>	
	<b>VS (d.nm)</b>	<b>%EE</b>
Lipoid S-100	Large vesicles were formed, visible by naked eyes	
Lipoid S-75	210.2 ± 5.98	33.18 ± 1.66
DPPC	Large vesicles were formed, visible by naked eyes	
Phospholipon 90H	256.9 ± 7.43	27.50 ± 0.98
DSPC	326.3 ± 9.70	20.16 ± 2.32
Phospholipon 80H	262.6 ± 8.26	21.92 ± 2.84
Lipoid S-75: DSPC::1:1	358.2 ± 18.14	25.37 ± 1.52
Phospholipon 90H: DSPC::1:1	376.6 ± 14.63	24.12 ± 1.68

(n=3, ± SD)

**6.16.3. Screening and optimization of process parameters of lipid film formation:**

In ATO loaded glycosomes (chapter-5), process parameters for lipid film formulation, such as solvents, solvent evaporation temperature and time, vacuum condition, speed of rotation for film formation and hydration, etc., were optimised. For the preparation of RSNa loaded glycosomes, the same parameters were used (shown in table-6.6).

Table- 6.6. Optimized process parameter for lipidic thin film formation

<b>Parameters</b>	<b>Optimum values</b>
<b>Selection of organic phase</b>	Methanol: Chloroform (1:1)
<b>Solvent evaporation time</b>	30 min
<b>Solvent evaporation temperature</b>	60°C
<b>Vacuum condition</b>	400 mmHg
<b>Speed of rotation for film formation</b>	150 rpm
<b>Speed of rotation for film hydration</b>	150 rpm

**6.16.4. Screening and optimization of process parameter for preparation of glycosomes:**

Process parameters such as time of hydration, hydration volume, sonication time, sonication amplitude, sonication cycles, etc. were screened and optimized as follows:

**a. Selection of time of hydration:**

The time of hydration was optimized on the basis of visual observation of complete removal and hydration of lipidic film. For the formation of proper vesicle orientation, sufficient time was required. The shorter time upto 30 min resulted in improper removal of film from wall of flask. At 60 minutes and higher, the film was completely removed from the wall of the flask and a homogeneously dispersed in hydration medium (as shown in table- 6.7). On the basis of results, 60 minutes was selected as optimum time of hydration for further development.

**b. Selection of hydration volume:**

The hydration volume was selected on the basis of complete removal of lipid film. A 5 mL volume of hydration was sufficient for complete removal of film from the flask wall and dispersion in hydration medium (shown in table-6.7). Thus, 5 mL of hydration medium was chosen as optimum volume of hydration for further development.

**c. Selection of hydration medium:**

Distilled water and phosphate buffer (PBS) pH 7.4 with glycerol were tested for hydration of lipid film. The results showed that, in comparison to PBS pH 7.4, maximum quantity of drug was entrapped in glycosomes using distilled water as the hydrating medium with a low vesicle size (shown in the table- 6.7). Thus, distilled water containing glycerol (20%w/w) was used as hydrating medium for further development.

**d. Selection of pulse of sonication cycle:**

For size reduction, the multilamellar vesicles were subjected to probe sonication. The sonication parameters had a significant influence on vesicle size and entrapment efficiency. Because it permits MLVs to be converted into SUVs, the cycle must be kept in ON-OFF mode. As a result, the vesicular layer develops, which incorporates the medication within the layer. According to the finding (shown in the table- 6.7), a 5 sec ON, 5 sec OFF sonication cycle produced large vesicles, whereas a 2 sec ON, 2 sec OFF sonication cycle produced vesicles with a  $208.7 \pm 7.70$  d.nm of vesicle size and  $32.02 \pm 2.39$  % EE. Thus, a 2 sec ON, 2 sec OFF pulse of the sonication cycle was chosen for further development.

**e. Selection of amplitude of sonication:**

Probe-sonication is an effective and widely used approach for reducing vesicle size and improving vesicle uniformity. The impact of probe-sonication process parameters on drug EE and VS of glycosomes must be evaluated, and the probe-sonication condition must be optimised for high drug EE. The amplitude of sonication showed significant influence on vesicle size and entrapment efficiency. On the basis of results, it was shown that increase in amplitude decreases vesicle

size. While increases in amplitude caused an increase in entrapment efficiency up to 60%, beyond that, decreases in entrapment efficiency and increase in vesicle size were observed. On the basis of preliminary screening results, 40-60 % amplitude was selected for further optimization.

**f. Selection of sonication cycles:**

Sonication is a reasonably simple method for obtaining unilamellar glycosomes with diameters less than 200 nm. The sonication cycle number had significant effects on vesicle size and entrapment efficiency. The results of preliminary screening showed decrease in vesicle size and increase in entrapment efficiency with increase in sonication upto 30 cycles. Further increase in the sonication cycle upto 35 leads to an increase in vesicle size and a decrease in entrapment efficiency. Hence, the selected range for further optimization for sonication cycles was 15-30 cycles.

Table- 6.7. Effect of process parameters for preparation of glycosomes

<b>Time of hydration</b>		
<b>Time (min)</b>	<b>Observation</b>	
30	Inefficient hydration, not complete removal of film	
60	Complete hydration and removal of film with homogenous dispersion of glycosomes.	
75	Complete hydration with homogenous dispersion.	
<b>Hydration volume</b>		
<b>Volume (mL)</b>	<b>Observation</b>	
5	Complete removal of film	
7.5	Complete removal of film	
10	Complete removal of film	
<b>Hydration medium</b>		
<b>Medium containing</b>	<b>Observation</b>	
	<b>Vesicle size (d.nm)</b>	<b>Entrapment efficiency (%)</b>
glycerol		
Distilled water	289.1 ± 9.40	28.80 ± 0.93

PBS pH 7.4	208.8 ± 4.81	32.02 ± 1.89
<b>Pulse of sonication Cycles</b>		
Pulse of sonication Cycles	Observations	
	Vesicle size (d.nm)	Entrapment efficiency (%)
5 Sec ON, 5 Sec OFF	Large vesicles were formed which were visible by naked eyes	
2 Sec ON, 2 Sec OFF	208.8 ± 7.70	32.02 ± 1.39
<b>Amplitude of sonication</b>		
Amplitude of sonication (%)	Observations	
	Vesicle size (d.nm)	Entrapment efficiency (%)
20	603.2 ± 7.81	34.83 ± 2.48
30	444.5 ± 4.48	42.27 ± 1.63
40	258.7 ± 4.87	55.53 ± 1.74
50	201.1 ± 6.20	46.79 ± 1.35
60	185.1 ± 5.74	60.85 ± 1.78
70	493.0 ± 5.46	38.22 ± 1.00
<b>Cycles of sonication</b>		
Cycles of sonication	Observations	
	Vesicle size (d.nm)	Entrapment efficiency (%)
10	340.9 ± 7.19	30.80 ± 1.10
15	253.4 ± 4.47	45.26 ± 2.06
20	246.2 ± 4.93	46.67 ± 2.18
25	195.6 ± 7.92	62.20 ± 1.80
30	185.1 ± 6.23	60.85 ± 0.74
35	313.5 ± 3.86	57.86 ± 1.49

The table-6.8 displays the optimised process variables for formulating RSNa loaded glycerosomes that were kept constant during preliminary studies. The high-risk parameters were optimised while keeping these variables constant using surface response methodology.

Table- 6.8. Process variables for preparation of RSNa loaded glycosomes

Parameters	Optimum values
Time of hydration	60 min
Hydration volume	5 mL
Pulse of sonication cycle	2 sec ON, 2 sec OFF
Hydration medium	Distilled water

#### 6.16.5. Screening and optimization of formulation parameters on glycosomes preparation:

The screening and optimization of formulation parameters such as lipid:drug, cholesterol: drug, glycerol concentration etc. are shown table- 6.9:

##### a. Screening of lipid:drug molar ratio:

The lipid mole ratio with drug was varied from 2:1 to 9:1, and the effect on vesicle size and entrapment efficiency was studied. The lipid:drug molar ratio significantly altered the vesicle size and entrapment efficiency. The results showed that an increased lipid:drug ratio leads to an increase in VS and % EE upto 6:1, beyond which an increase in ratio decreases % EE. This might be due to the formation of lipid aggregation and clusters at high lipid:drug ratio, which can lead to a decrease in available vesicle cores for the entrapment of drug. From the results, 3:1 to 6:1 mole ratio of lipid to drug was selected for further development.

##### b. Screening of cholesterol:drug molar ratio:

Incorporating cholesterol in preparation of vesicular formulation is very important for the structure of vesicles, as it improves lipid packing and vesicle stability. The concentration of cholesterol has a significant impact on vesicle size and drug entrapment. Increase in the cholesterol:drug ratio up to 1:1 resulted in increased entrapment efficiency, whereas increase in cholesterol:drug ratio beyond that resulted in decreased %EE. This might be because at higher cholesterol concentrations, the bilayer hardens, which decreases the incorporation of drug into the vesicle core. The cholesterol mole ratio with drug of 0:1 to 1:1 was therefore selected for further optimization.

**c. Screening of concentration of glycerol:**

The effect of the concentration of glycerol on vesicle size and entrapment efficiency was studied. The increase in concentration of glycerol increased vesicle size, which might be due to the sticky nature of glycerol [21]. The increased concentration of glycerol increased entrapment efficiency to a certain level; beyond that, a decrease in entrapment efficiency was observed with the increase in concentration of glycerol, which might be due to an increase in the viscosity of dispersion, which hindered size reduction and resulted in a reduction of the aqueous core available for encapsulation of drug [21]. Hence, based on minimum vesicle size and maximum entrapment efficiency, a 20% w/w glycerol concentration was selected for the further preparation of glycosomes.

Table- 6.9. Effect of formulation parameters on preparation of RSNa loaded glycosomes

<b>Screening of Lipid:drug molar ratio</b>		
<b>Lipid:drug molar ratio</b>	<b>Observations</b>	
	<b>VS (d.nm)</b>	<b>% EE</b>
2:1	155.3 ± 5.61	28.69 ± 2.36
3:1	208.8 ± 5.45	32.02 ± 1.17
4:1	217.3 ± 7.71	49.54 ± 1.29
6:1	185.1 ± 6.59	60.85 ± 1.11
9:1	390.1 ± 8.36	63.99 ± 0.56
<b>Screening of Cholesterol:drug molar ratio</b>		
<b>Cholesterol:drug molar ratio</b>	<b>Observations</b>	
	<b>VS (d.nm)</b>	<b>% EE</b>
0:1	213.9 ± 4.41	40.02 ± 1.86
0.25:1	249.1 ± 3.91	46.21 ± 1.30
0.50:1	216.3 ± 5.61	47.13 ± 1.84
0.75:1	160.8 ± 4.22	52.07 ± 0.85
1:1	185.1 ± 7.91	60.85 ± 1.68
1.5:1	260.9 ± 17.4	51.36 ± 2.69

Screening of glycerol concentration		
Glycerol concentration (%)	Observations	
	VS (d.nm)	% EE
5	170.6 ± 6.39	46.74 ± 1.30
10	192.0 ± 7.84	48.75 ± 1.86
20	185.1 ± 4.38	60.85 ± 1.30
30	204.9 ± 3.70	62.03 ± 1.89
40	594.5 ± 9.15	54.04 ± 1.47

The high-risk parameters were optimised while keeping other process and formulation factors constant using a design of experiment technique.

### 6.17. Definitive screening design for optimization of glycosomes

The influence of several process and formulation parameters on the quality of glycosomes was analysed by using Definitive Screening Design (DSD). The factors investigated for formulation were lipid:drug mole ratio, cholesterol:drug mole ratio, sonication amplitude, and sonication cycles. Vesicle size and entrapment efficiency were the responses used. Applying the statistical programme DesignExpert V.13.0, the experiment design's statistical analysis was completed (Stat-Ease, Inc., USA).

### 6.18. Design Matrix

DesignExpert software generated a randomised matrix of thirteen batches, as shown in table- 6.10.

Table- 6.10. Experimental runs and their results for RSNa loaded glycosomes

	Factor 1	Factor 2	Factor 3	Factor 4	Response 1	Response 2
Run	A: Lipid:drug Molar ratio	B: Cholesterol: drug Molar ratio	C: Amplitude (%)	D: Sonication cycle	VS (d.nm)	EE (%)
R1	6:1	0:1	50	15	198.8 ± 5.51	46.86 ± 1.89
R2	6:1	0:1	60	30	171.6 ± 6.36	52.72 ± 2.63
R3	3:1	0:1	40	30	140.7 ± 4.89	30.15 ± 2.01
R4	6:1	1:1	60	15	154.5 ± 6.93	54.73 ± 1.52
R5	4.5:1	0:1	40	15	200.2 ± 8.15	45.41 ± 1.63
R6	6:1	0.5:1	40	30	150.7 ± 2.56	48.58 ± 1.83
R7	3:1	1:1	40	15	130.2 ± 4.36	35.61 ± 2.14
R8	6:1	1:1	40	22.5	168.2 ± 6.32	61.85 ± 1.42
R9	4.5:1	1:1	60	30	164.8 ± 2.56	52.79 ± 2.22
R10	3:1	0:1	60	22.5	179.2 ± 4.58	39.65 ± 1.36
R11	4.5:1	0.5:1	50	22.5	211.9 ± 9.25	50.97 ± 2.15
R12	3:1	0.5:1	60	15	135.7 ± 3.84	31.76 ± 2.18
R13	3	1	50	30	133.1 ± 4.58	33.16 ± 1.15

(n=3, ± S.D.)

The effect of independent variables on responses is discussed below:

### 6.18.1. Effect of independent variables on vesicle size:

Because of various independent factor combinations throughout all 13 experimental runs, the values of vesicle size varied from 130.2 to 211.9 d.nm. According to the statistical study, there was a strong connection between the actual and predicted values for vesicle size, with an  $R^2$  value of 0.9866.

#### ANOVA results of model:

Summary of the ANOVA results for vesicle size model is included in the table- 6.11 along with the model p-value and predicted and adjusted  $R^2$  values.

Table- 6.11. Summary of ANOVA results of different models for vesicle size

Source	Model p-value	Adjusted $R^2$	Predicted $R^2$	
<b>Design Model</b>	<b>0.0003</b>	<b>0.9836</b>	<b>0.9351</b>	<b>Recommended</b>
<b>Linear</b>	0.2723	0.1592	-0.2053	Suggested
<b>2FI</b>	0.7077	-0.1132	-0.3795	Aliased

The highest polynomial with the lowest p-value ( $p < 0.05$ ) was considered for model selection (shown in table- 6.11). Based on the criteria, a design model was recommended to be best fitted to the observed responses. Other models were not suitable for prediction either due to a low  $R^2$  value or a high p value as compared to the design model.

ANOVA results of design model for vesicle size is shown in table- 6.12. The model was potentially significant given the Model F-value of 90.87. The F-value this large might happen owing to noise only 0.03% of the total. Model terms are considered significant when the P-value is less than 0.0500. A, B, D,  $A^2$ ,  $B^2$ ,  $C^2$ , and  $D^2$  were significant terms in this model. The F value of factor A and factor B was highest (129.18 and 161.61 respectively) i.e., maximum effect on vesicle size, while factor C and D have low effect on vesicle size on the basis of F value.

Table- 6.12. ANOVA results of design model for vesicle size

Source	Sum of Squares	df	Mean Square	F-value	p-value	
<b>Model</b>	8778.39	8	1097.30	90.87	0.0003	Significant
<b>A-Lipid:drug molar ratio</b>	1560.00	1	1560.00	129.18	0.0003	
<b>B-Cholesterol:drug molar ratio</b>	1951.61	1	1951.61	161.61	0.0002	
<b>C-Amplitude</b>	24.96	1	24.96	2.07	0.2239	
<b>D-Sonication cycle</b>	342.22	1	342.22	28.34	0.0060	
<b>A<sup>2</sup></b>	2248.45	1	2248.45	186.19	0.0002	
<b>B<sup>2</sup></b>	121.28	1	121.28	10.04	0.0339	
<b>C<sup>2</sup></b>	520.37	1	520.37	43.09	0.0028	
<b>D<sup>2</sup></b>	1178.83	1	1178.83	97.62	0.0006	
<b>Residual</b>	48.30	4	12.08			
<b>Cor Total</b>	8826.70	12				

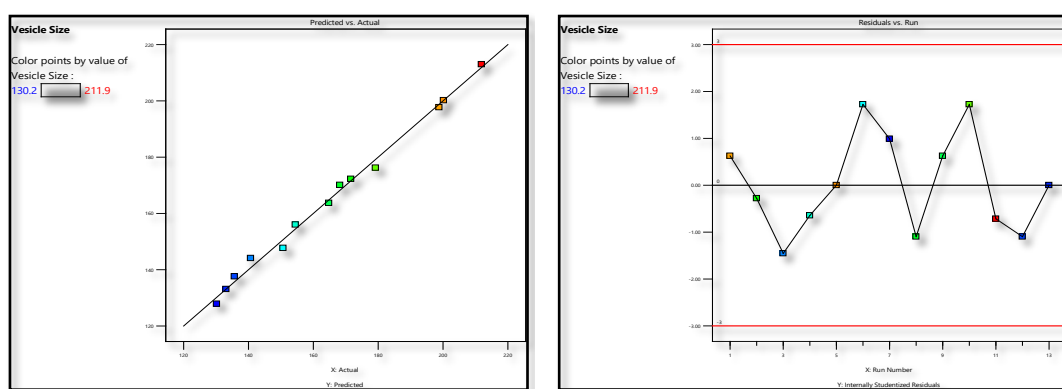
Table- 6.13. Summary of ANOVA results for vesicle size

Parameters	Results	Parameters	Results
<b>Std. Dev.</b>	3.48	<b>R<sup>2</sup></b>	0.9945
<b>Mean</b>	164.58	<b>Adjusted R<sup>2</sup></b>	0.9836
<b>C.V. %</b>	2.11	<b>Predicted R<sup>2</sup></b>	0.9351
		<b>Adeq Precision</b>	29.4357

The difference between the Predicted R<sup>2</sup> of 0.9351 and the Adjusted R<sup>2</sup> of 0.9836 was less than 0.2, which is considered to be an acceptable agreement. The signal-to-noise ratio is determined by using Adeq Precision. A ratio of at least 4 is preferred. The signal is strong enough based on your ratio of 29.4357. This model is useful for navigating the design space.

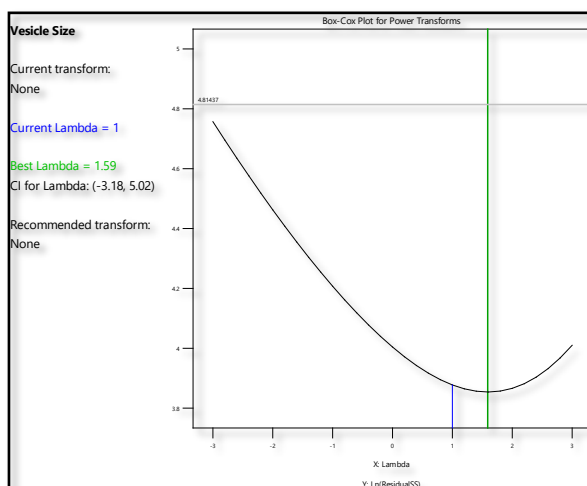
**Model diagnostic plots:**

Figure- 6.2 depicts several diagnostic graphs for model evaluation. The **expected vs. real plot** (a) follows a 45° straight line, indicating a tight match between actual and predicted values. The **residual versus run plot** (b) in the current study displays a random distribution of residuals, indicating that there was no relationship of residual with time and the absence of any time dependent variable. The **Box-Cox plot** (c) revealed a current  $\lambda$  value of 1, which is closer to the best  $\lambda$  values (1.59) and found inside the 95% CI for  $\lambda$  i.e., -3.18 to 5.02, suggested that no power transformation was necessary.



a. Plot of predicted Vs Actual

b. Plot of residuals Vs run

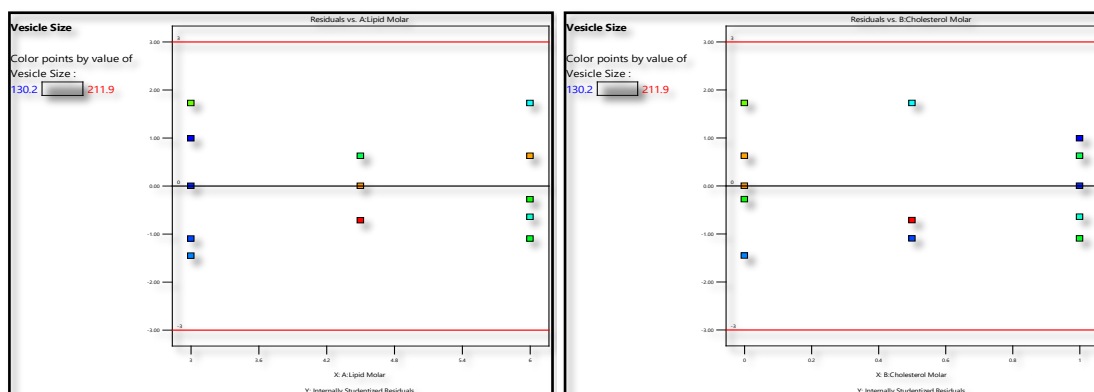


c. Box-Cox plot for power transformation

Figure- 6.2. Various model diagnostic plots for vesicle size

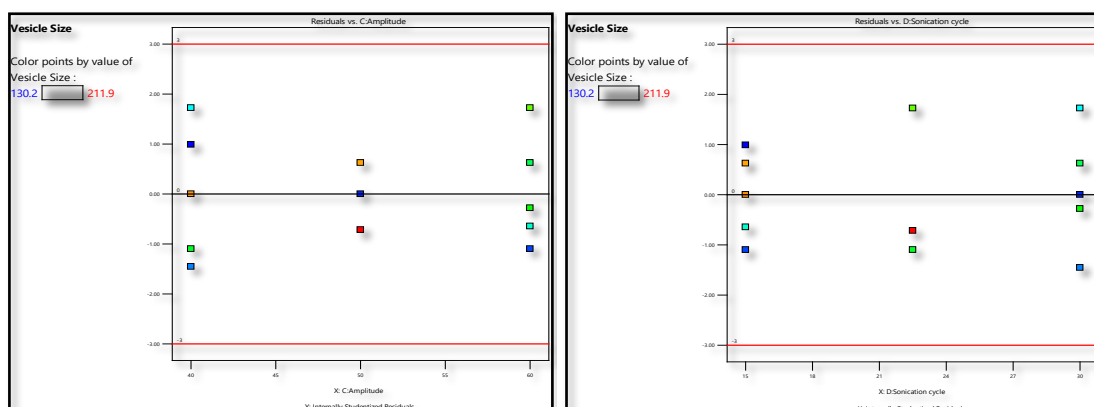
- Plot of predicted Vs Actual
- Plot of residuals Vs run
- Box-Cox plot for power transformation

The residual plots for each factor (shown in figure-6.3) exhibit a random dispersion over increasing levels of factor, demonstrating that the model is efficient in accounting for the variation for each factor.



a. Residuals Vs Lipid:drug molar ratio

b. Residuals Vs Cholesterol:drug molar ratio



c. Residuals Vs Amplitude

d. Residuals Vs Sonication cycle

Figure- 6.3. Residual Vs factor plots

- Residuals Vs Lipid:drug molar ratio
- Residuals Vs Cholesterol:drug molar ratio
- Residuals Vs Amplitude
- Residuals Vs Sonication cycle

The plot (shown in figure- 6.4) showed that lipid:drug molar ratio and amplitude have a positive remarkable influence on vesicle size, as revealed by an increase in vesicle size with an increase in lipid:drug molar ratio and amplitude.

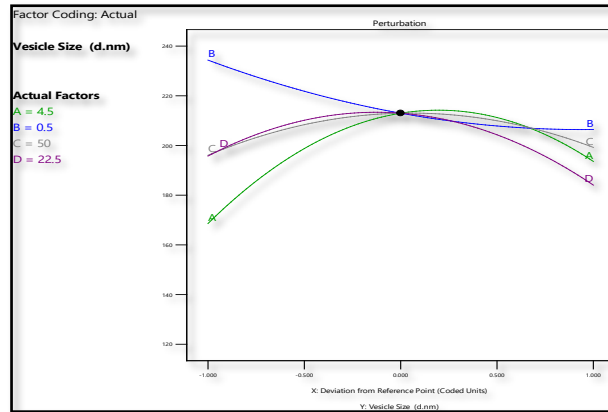


Figure- 6.4. Pipel's plot on response variable 1

**Model plots: Response surface plot (3D plot):**

The ANOVA value informs us about the variables that have a significant influence on vesicle size, as seen in the 3D graphs. The red area in the figure-6.5 represents the largest vesicle size, while the blue area represents the smallest vesicle size.

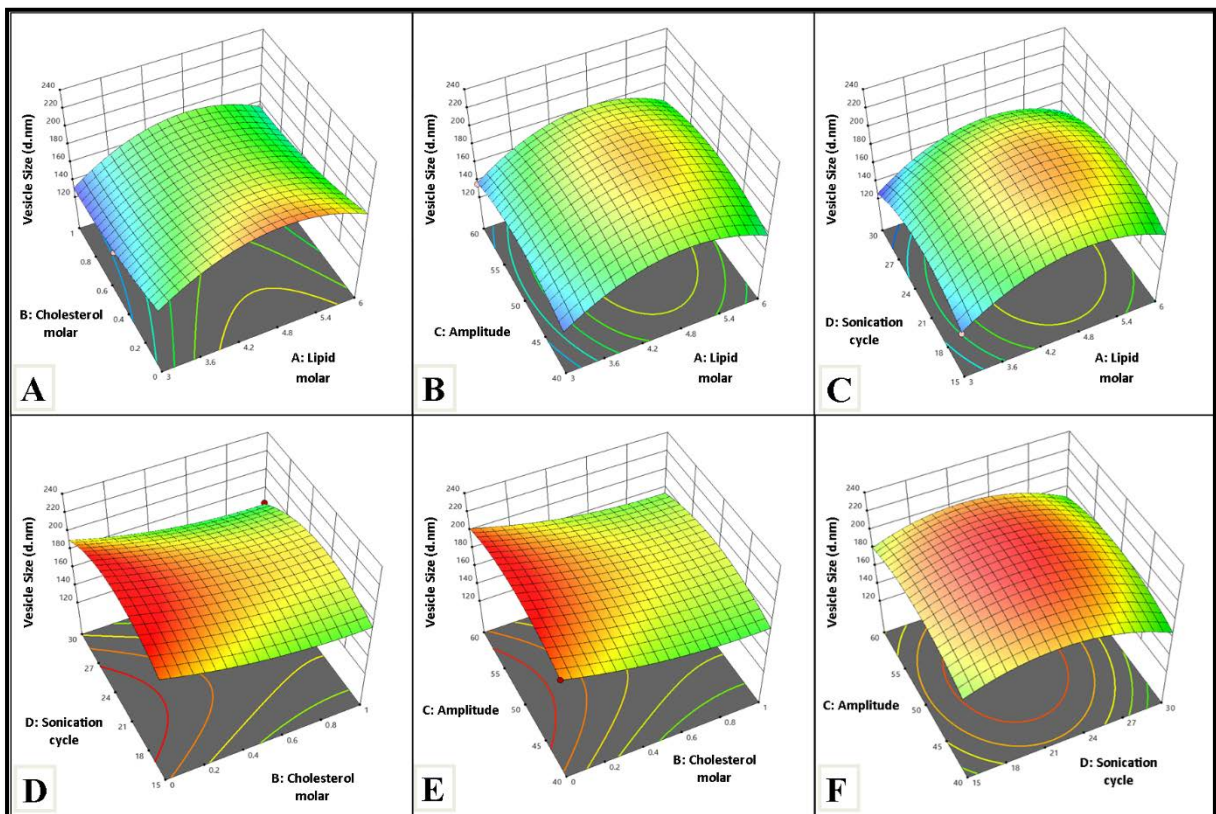


Figure- 6.5. Response surface plot (3D) showing combined effect of independent variables on vesicle size

- (a)- Combined effect of Lipid:drug molar ratio and Cholesterol:drug molar ratio
- (b)- Combined effect of Lipid:drug molar ratio and Amplitude

- (c)- Combined effect of Sonication cycle and Lipid:drug molar ratio
- (d)- Combined effect of Sonication cycle and Cholesterol:drug molar ratio
- (e)- Combined effect of Amplitude and Cholesterol:drug molar ratio
- (f)- Combined effect of Sonication cycle and Amplitude

Response surface plot (3D) showing combined effect of independent variables on vesicle size is shown in figure- 6.5. Equation-6.5 denoted that the magnitude of factor A and C showed a positive effect on vesicle size, while factor B and D showed a negative effect on vesicle size.

From the 3D surface plot, it was revealed that the lipid:drug molar ratio showed positive effects on vesicle size, indicating an increase in vesicle size with an increase in the lipid:drug molar ratio. The magnitude of the cholesterol:drug molar ratio denoted that an increase in the cholesterol:drug molar ratio decreases vesicle size. It is reported that cholesterol increases the chain order of the lipid bilayer of vesicular systems, resulting in close packing and consequently reduced size [1, 22]. The magnitude of the amplitude of sonication indicated that an increase in amplitude results in an increase in vesicle size due to the higher amplitude, which causes an elevation in the temperature of vesicular dispersion due to high energy acquisition during the sonication process. Too strong probe sonication leads to disruption of vesicular structure and degradation of lipid, resulting in an increase in vesicle size. The magnitude of the number of sonication cycles indicates that the increased number of sonication cycles results in a decrease in vesicle size. The decrease in vesicle size becomes faster by increasing the number of sonication, as is expected due to the conversion of large lamellar vesicles to small bilayer vesicles [23, 24]. The fluidity of vesicles made it possible for the lipid molecules to rearrange and reassemble to produce smaller vesicles under optimal probe-sonication conditions.

Polynomial equation for vesicle size:

The polynomial equations were obtained from design for vesicle size as follows:

Final equation in terms of coded factors:

$$\text{Vesicle Size (d.nm)} = + 212.99 + 12.49 * A - 13.97 * B + 1.58 * C - 5.85 * D - 31.89 * A^2 + 7.41 * B^2 - 15.34 * C^2 - 23.09 * D^2$$

.....equation- 6.5.

Reduced equation in terms of coded factors:

$$\text{Vesicle Size (d.nm)} = + 212.99 + 12.49 * A - 13.97 * B - 5.85 * D - 31.89 * A^2 + 7.41 * B^2 - 15.34 * C^2 - 23.09 * D^2$$

.....equation- 6.6.

### 6.18.2. Effect of independent variables on % EE:

The values of entrapment efficiency varied from 30 to 62 % throughout all 13 runs due to variation in independent factor combinations. From the statistical analysis, we observed that the  $R^2$  value for actual Vs predicted values for EE was found to be 0.9802 which was good correlation.

#### ANOVA results of model:

Summary of the ANOVA results of different models for % EE is shown in table-6.14 which depicts model p-value with adjusted and predicted  $R^2$  values.

Table- 6.14. Summary of ANOVA results of different models for % EE

Source	Model p-value	Adjusted $R^2$	Predicted $R^2$	
Design Model	< 0.0001	0.9909	0.9802	<b>Recommended</b>
Linear	0.0074	0.6924	0.5017	<b>Suggested</b>
2FI	0.1896	0.8673	0.8344	<b>Aliased</b>

For model selection, the polynomial with the lowest p values (0.05) and highest  $R^2$  value has been used. Based on the criteria, the design model was determined to have the best fit to the observed responses and was chosen for further investigation.

Table- 6.15. ANOVA results of design model for % EE

Source	Sum of Squares	df	Mean Square	F-value	p-value	
<b>Model</b>	1200.05	8	150.01	163.73	< 0.0001	<b>Significant</b>
<b>A-Lipid:drug molar ratio</b>	891.32	1	891.32	972.88	< 0.0001	
<b>B- Cholesterol:drug molar ratio</b>	54.52	1	54.52	59.51	0.0015	
<b>C-Amplitude</b>	10.10	1	10.10	11.02	0.0294	
<b>D-Sonication cycle</b>	0.9181	1	0.9181	1.00	0.3735	
<b>A<sup>2</sup></b>	79.56	1	79.56	86.84	0.0007	
<b>B<sup>2</sup></b>	18.99	1	18.99	20.72	0.0104	
<b>C<sup>2</sup></b>	21.12	1	21.12	23.05	0.0086	
<b>D<sup>2</sup></b>	129.34	1	129.34	141.18	0.0003	
<b>Residual</b>	3.66	4	0.9162			
<b>Cor Total</b>	1203.72	12				

ANOVA results of design model for % EE is shown in table- 6.15. The model's F-value of 163.73 indicates that it is significant. An F-value this big might occur owing to noise just 0.01% of the time. The model terms with P-values less than 0.0500 are significant. A, B, C, A<sup>2</sup>, B<sup>2</sup>, C<sup>2</sup>, and D<sup>2</sup> were significant model terms in this case.

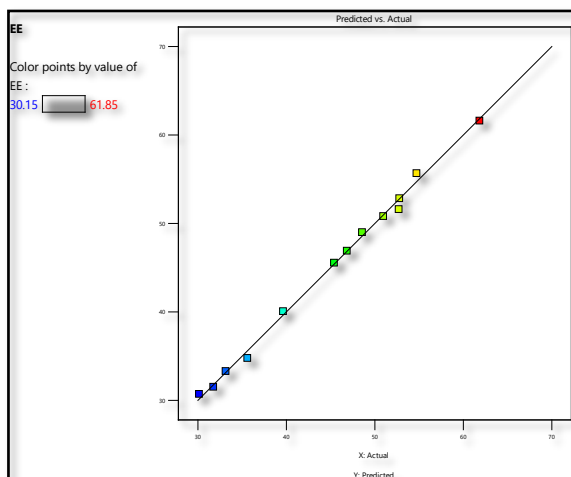
Table- 6.16. Summary of ANOVA results for % EE

Parameters	Values	Parameters	Values
<b>Std. Dev.</b>	0.9572	<b>R<sup>2</sup></b>	0.9970
<b>Mean</b>	44.94	<b>Adjusted R<sup>2</sup></b>	0.9909
<b>C.V. %</b>	2.13	<b>Predicted R<sup>2</sup></b>	0.9802
		<b>Adeq Precision</b>	38.7968

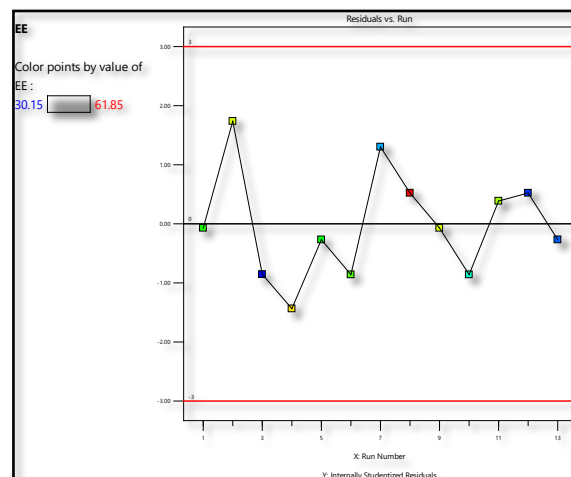
The Predicted R<sup>2</sup> of 0.9802 is relatively close to the Adjusted R<sup>2</sup> of 0.9909, with a difference of less than 0.2 (shown in table- 6.16). The signal-to-noise ratio is measured

using the Adeq Precision. A ratio larger than 4 is preferred. The signal-to-noise ratio of 38.7968 suggests a sufficient signal. This model is useful for navigating the design space.

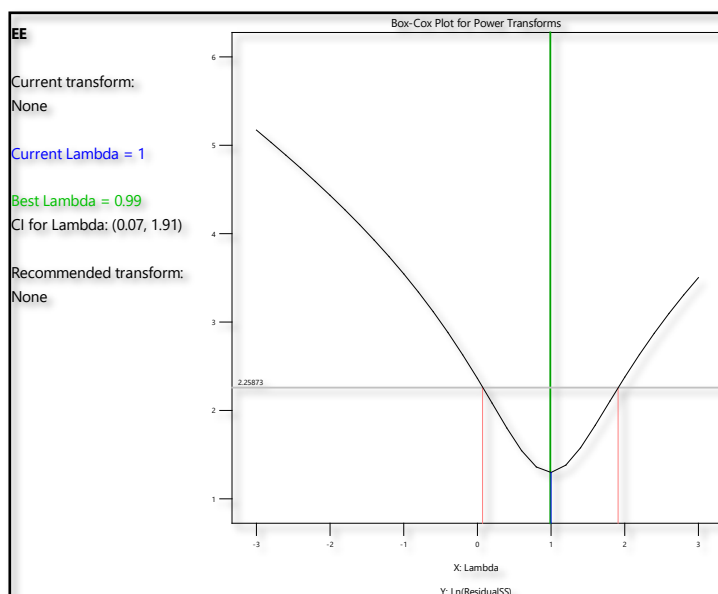
### Model diagnostics plot:



a. Plot of actual Vs predicted



b. Plot of residual Vs run



c. Box-Cox plot for power transformation

Figure- 6.6. Various model diagnostic plots

- Plot of actual Vs predicted
- Plot of residual Vs run
- Box-Cox plot for power transformation

Various diagnostic plots for evaluation of model are shown in figure- 6.6. The **predicted vs actual plot** (figure-6.6a) follows a 45° straight line which indicates a close estimation of actual values with predicted values. The **residual vs run plot** (figure-6.6b) shows a random distribution of residuals in the current analysis, indicating that there was no association of residual with time and the absence of a lurking dependent variable. The **Box-Cox plot** (figure-6.6c) showed that the  $\lambda$  value of 1, which lies nearer to the best  $\lambda$  values and found within 95% CI of it, indicated that there was no required power transformation.

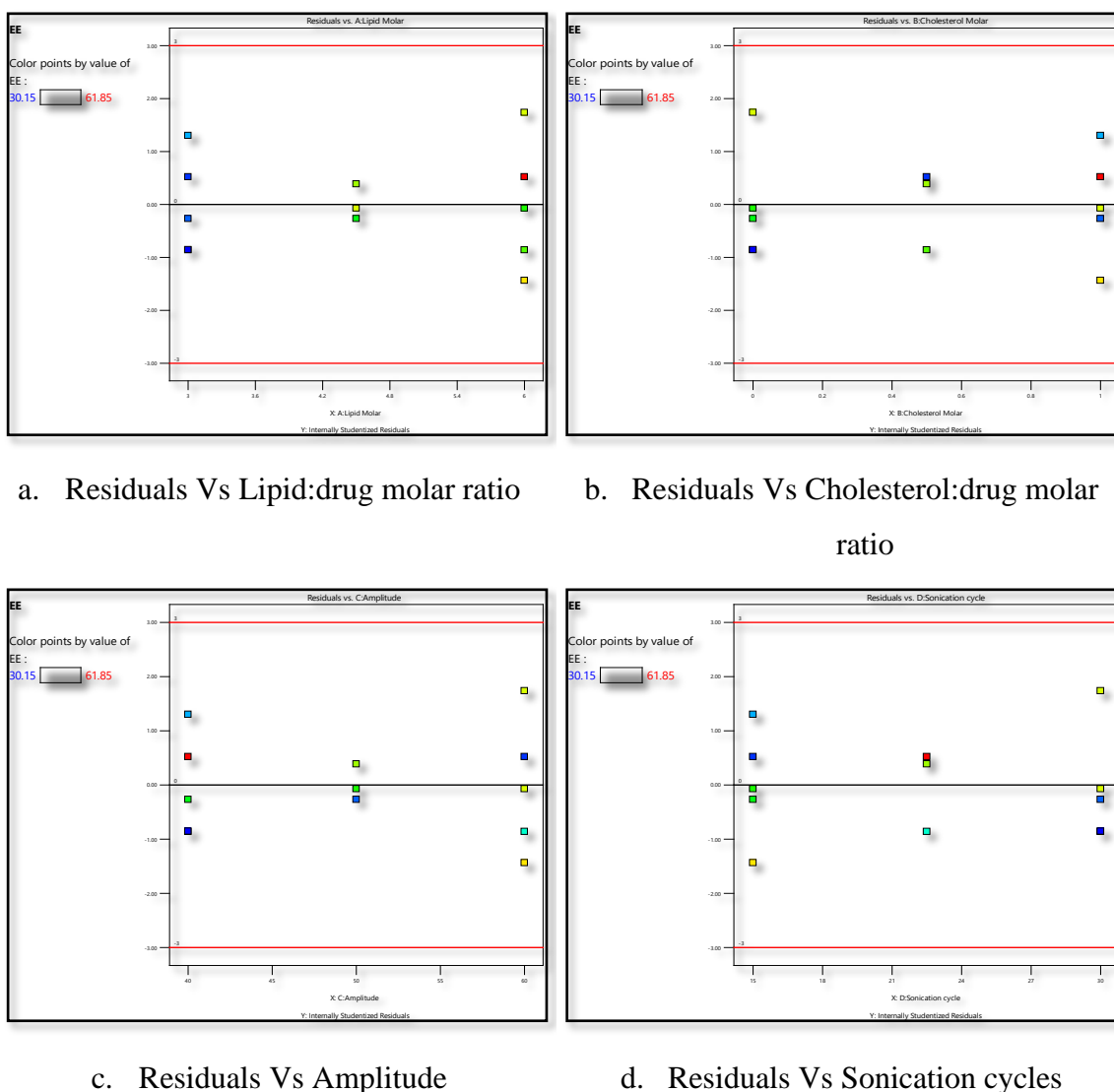


Figure- 6.7. Residuals Vs each factors plots

- Residuals Vs Lipid:drug molar ratio
- Residuals Vs Cholesterol:drug molar ratio
- Residuals Vs Amplitude
- Residuals Vs Sonication cycles

The plots for residuals with each factor (shown in figure- 6.7) represents a random scattering over increasing levels of factor indicating that the model is effective in accounting for the variance for each factor.

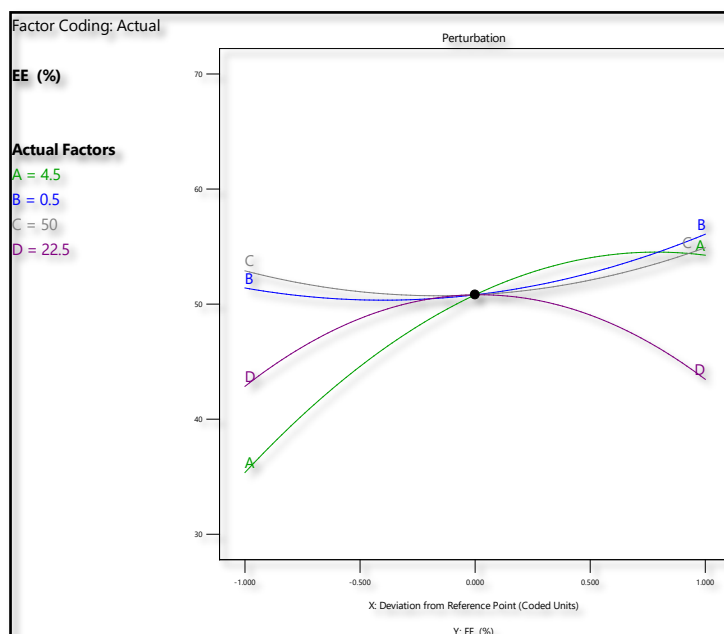


Figure- 6.8. Pipel's plot on response variables 2

The Pipel's plot on the response of % EE (figure- 6.8) showed that increased lipid:drug molar ratio, cholesterol:drug molar ratio and the amplitude of sonication increased entrapment efficiency, which indicates positive effects.

## Model plots: Response surface 3D plots

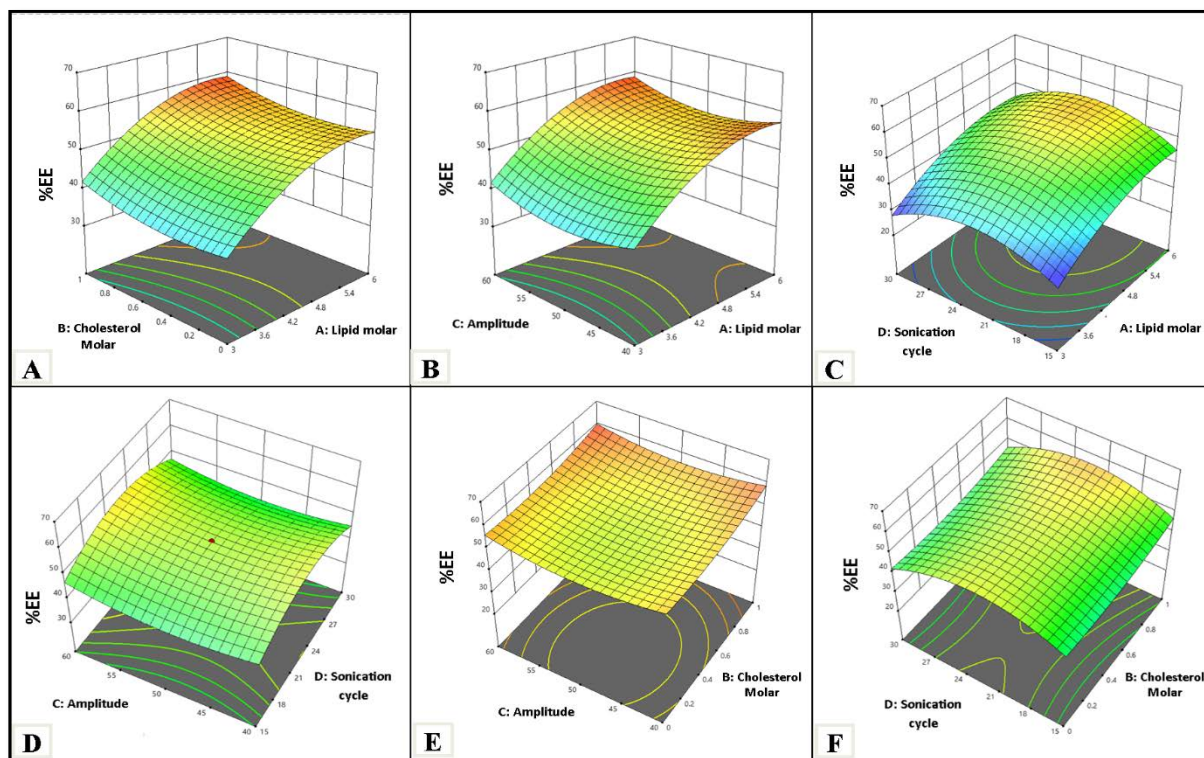


Figure- 6.9. Response surface plot (3D) showing combined effect of independent variables on % EE

- (A)- Combined effect of Lipid:drug molar ratio and Cholesterol:drug molar ratio
- (B)- Combined effect of Lipid:drug molar ratio and Amplitude
- (C)- Combined effect of Sonication cycle and Lipid:drug molar ratio
- (D)- Combined effect of Sonication cycle and Amplitude
- (E)- Combined effect of Amplitude and Cholesterol:drug molar ratio
- (F)- Combined effect of Sonication cycle and Cholesterol:drug molar ratio

The figure-6.9 shows 3D surface response plot of combined effects of different variables on response i.e., % EE. The equation-6.7 denoted that the magnitude of factor A, B, C and D showed a positive effect on entrapment efficiency, indicating an increase in factor A, B, C and D resulted in an increase in %EE.

The magnitude of factor A showed synergistic effects on entrapment efficiency, denoting an increase in EE with an increase in the lipid:drug molar ratio due to the formation of the maximum number of vesicles, which enhanced the possibility for RSNa to be encapsulated into the internal core of vesicles surrounded by a lipid bilayer membrane [25]. This finding coincides with that proposed by Zhang et al. (2017), who

endorsed that increasing phospholipid concentration increased paeoniflorin % EE in glycosomal vesicles [3]. The magnitude of factor B showed positive effects on % EE, indicating that an increased cholesterol molar ratio increases the entrapment efficiency, which might be attributed to the increased amounts of cholesterol filling the free spaces within the lipid chains, which attenuates molecular mobility [26]. The magnitude of factor C and factor D showed a positive effect on entrapment efficiency, indicating an increase in sonication amplitude and cycles, which resulted in an increase in %EE. When the sonication amplitude and cycles were increased, it resulted in the formation of the maximum number of vesicles, which allowed more drug to be encapsulated in the internal core of the vesicle and resulted in a higher EE [23].

The polynomial equations were obtained from design for entrapment efficiency as follows:

Final equation in terms of coded factors:

$$\begin{aligned} \text{Entrapment Efficiency} & + 50.81 + 9.44 * A + 2.34 * B + 1.01 * C \\ (\%) = & + 0.3030 * D - 6.00 * A^2 + 2.93 * B^2 + \\ & 3.09 * C^2 - 7.65 * D^2 \end{aligned}$$

.....equation- 6.7.

Reduced equation in terms of coded factors:

$$\begin{aligned} \text{Entrapment Efficiency} & + 50.81 + 9.44 * A + 2.34 * B + 1.01 * C \\ (\%) = & - 6.00 * A^2 + 2.93 * B^2 + 3.09 * C^2 - 7.65 \\ & * D^2 \end{aligned}$$

.....equation- 6.8.

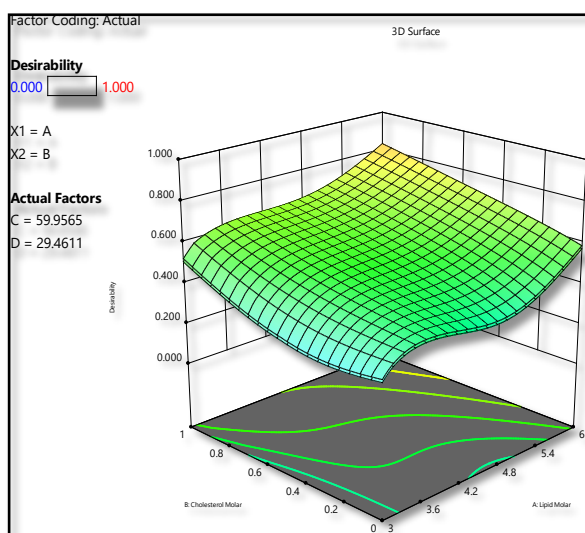
### 6.19. Desirability plot and overlay plot for optimization:

A desirability plot showed the optimal values for variables to get the desired results. The parameters for the desirability batch are listed in the table-6.17.

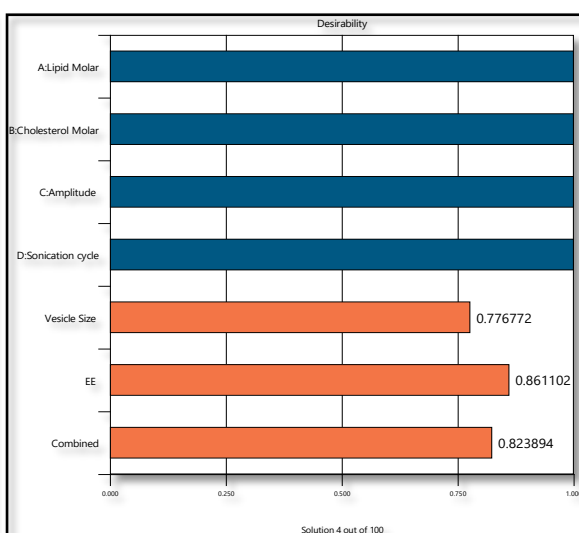
Table- 6.17. Variables for desirability plots and goals for response

Name of variable	Goal	Lower Limit	Upper Limit
<b>A:Lipid:drug molar ratio</b>	Range	3:1	6:1
<b>B:Cholesterol:drug molar ratio</b>	Range	0:1	1:1
<b>C:Amplitude</b>	Range	40	60
<b>D:Sonication cycle</b>	Range	15	30
<b>Vesicle Size (d.nm)</b>	Minimize	130.2	211.9
<b>EE (%)</b>	Maximize	30.15	61.85

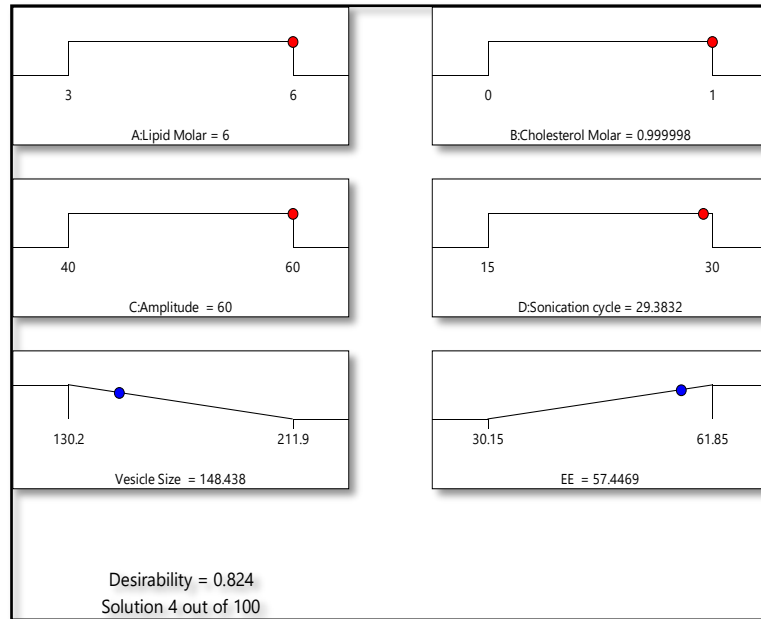
To carry out optimization using mathematical functions, desirability criteria and a desirability plot were devised. Higher and lower desired response values were determined for this, and software generated variable values to assist in producing the desired response. The ramp graph (figure-6.10c) depicts predicted R1 and R2 values for the optimal concentration of independent variables, whereas the bar graph (figure-6.10b) depicts individual demand for R1 and R2. The proposed solution has a composite desirability of 0.823 (shown in figure- 6.10).



a. 3D Desirability plot



b. Bar graph of desirability



c. Ramp graph of desirability

Figure- 6.10. Desirability plot for RSNa loaded glycosomes

- 3D desirability plot
- Bar graph of desirability
- Ramp graph of desirability

To assess the desirability, RSNa-loaded glycosomes formulation was made according to the suggested batch, and the obtained response values were found to be comparable to the predicted responses (shown in table-6.18). Furthermore, the error of the design was found to be less than 5%, confirming its predictability. This demonstrates that the optimal formulation suggested by software is trustworthy for practical purposes.

Table – 6.18. Predicted and observed responses of optimized RSNa loaded glycosomes

Variables	Values	Responses	Predicted values	Observed values	% Error
<b>Lipid:drug molar ratio</b>	6.00:1	<b>Vesicle size (d.nm)</b>	148.44	153.8 ± 4.48	3.61
<b>Cholesterol:drug molar ratio</b>	0.99:1	<b>EE (%)</b>	57.44	59.75 ± 1.21	4.02
<b>Amplitude</b>	60.00				
<b>Cycles of sonication</b>	29.38				

(n=3, ± S.D.)

The observed values received were remarkably similar to the predicted values obtained from the check point batch, which is acceptable with % error. The predicted and observed values do not differ substantially at  $p > 0.05$ , indicating that the optimization technique is reliable.

#### 6.20. Graphical optimization to generate control space:

Figure-6.11 shows an overlay plot of the design. This overlay plot was generated by superimposing contour plots of both responses in the factor space, which displaces the region of feasible response values. The upper and lower ranges of the desired responses were selected for the generation of the overlay plot. The overlay plot shows how response variables relate to two continuous design variables i.e. lipid:drug molar ratio and cholesterol: drug molar ratio, while holding the other two variables i.e. amplitude and cycles of sonication at 60 % and 29.38 respectively. The yellow area inside each plot shows the range of independent variables where the criteria for both response variables are satisfied.

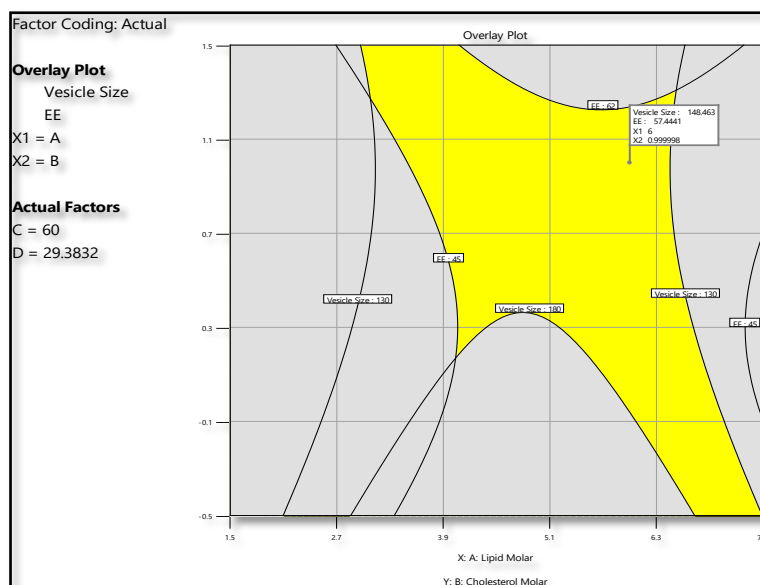


Figure – 6.11. Overlay plot for design space

### 6.21. Analysis of design space:

Figure- 6.12 and table-6.19 represents analysis of check point batches generated from design space. The analysis of the design space was done by picking three different batches randomly from the yellow region and preparing them using the variables suggested in it, and the predicted values of responses were compared with the observed values.

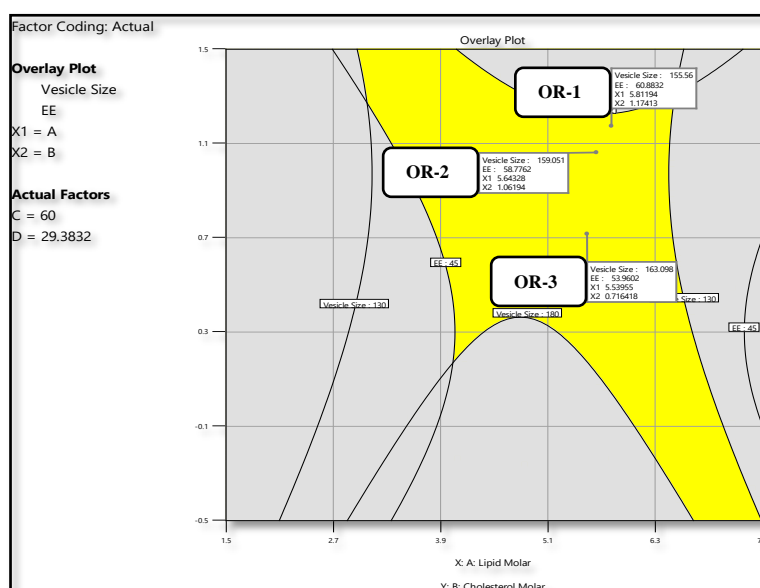


Figure – 6.12. Analysis of design space

Table- 6.19. Check point batch analysis

Formulations	Parameters	Predicted	Observed	Std. Error
OR-1	VS (d.nm)	155.56	156.6 ± 3.61	0.66
	% EE	60.88	58.36 ± 1.89	4.14
OR-2	VS (d.nm)	159.05	161.9 ± 5.96	1.79
	% EE	58.77	57.82 ± 2.02	1.61
OR-3	VS (d.nm)	163.09	167.1 ± 4.85	2.45
	% EE	53.96	55.75 ± 2.56	3.31

(n=3, ± S.D.)

According to the robustness analysis, the observed responses remained within the boundary, and the observed values were found to be closer to the predicted values.

## 6.22. Point prediction and confirmation:

The optimal response values were validated by doing the experiment in triplicate with the selected factor values. Based on the results (table-6.20), it was determined that the observed and predicted values were in excellent agreement, indicating the appropriateness of the chosen model for optimization.

Table – 6.20. Predicted responses for selected solution along with standard deviation

Responses	Predicted Mean	Observed mean	Std Dev	n	SE Pred	95% PI low	95% PI high
VS (d.nm)	148.44	153.8 ± 4.48	3.47	3	3.20	139.54	157.32
EE (%)	57.44	59.75 ± 1.21	0.96	3	0.88	54.99	59.89

(n=3, ± S.D.)

## 6.23. Physicochemical characterization of optimized batch:

### 6.23.1. Vesicle size, PDI and zeta potential determination:

The average vesicle size and polydispersity index of optimized batch was found to be 153.8 ± 4.48 d.nm and 0.213 ± 0.035 respectively. The zeta potential of optimized

batch was found to be  $-18.3 \pm 1.00$  mV. The negatively charged vesicular formulations strongly improve skin permeation of drugs in transdermal delivery [10, 27].

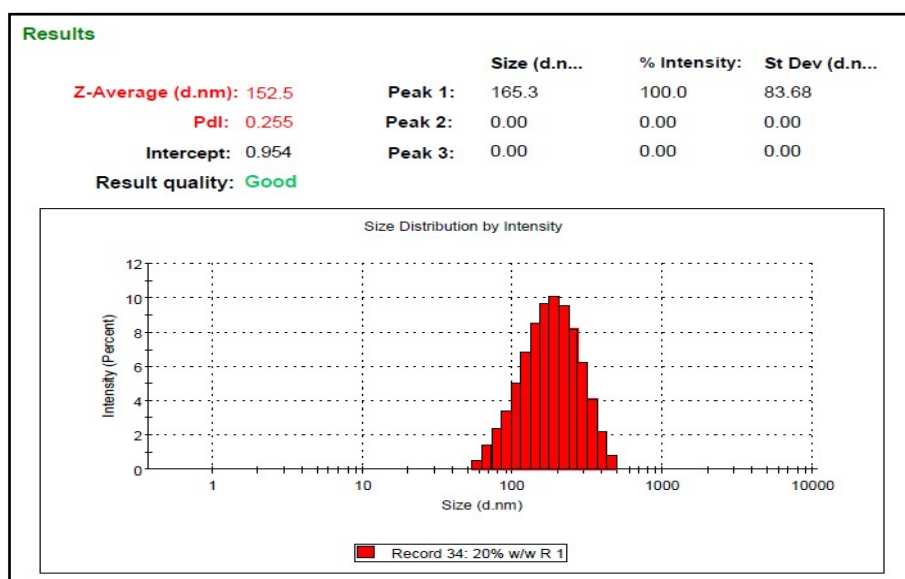


Figure- 6.13. Vesicle size measurement by zetasizer.

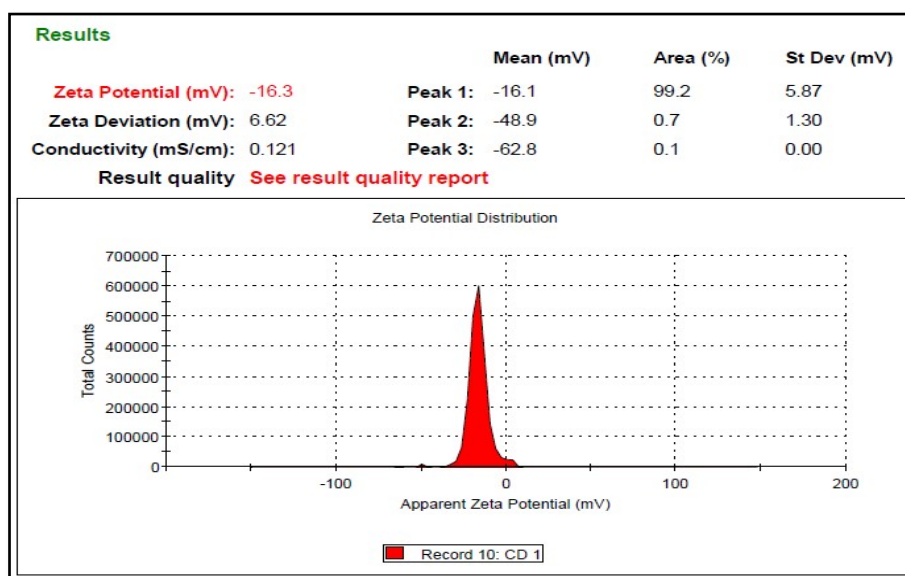


Figure- 6.14. Zeta potential analysis by zetasizer.

### 6.23.2. Entrapment efficiency and % DLC:

The % entrapment efficiency was found to be  $59.75 \pm 1.21$  % and drug loading capacity was found to be  $2.99 \pm 0.055$  %.

### 6.23.3. Morphological investigation:

The surface morphology of RSNa-loaded glycosomes is seen in the figure-6.15. The TEM image indicated smooth multilamellar vesicles ranging from 100 to 170 nm that are spherical in shape, small and uniform in size, are not agglomerated and are homogeneously dispersed in medium with no structural disturbances, confirming vesicle integrity.

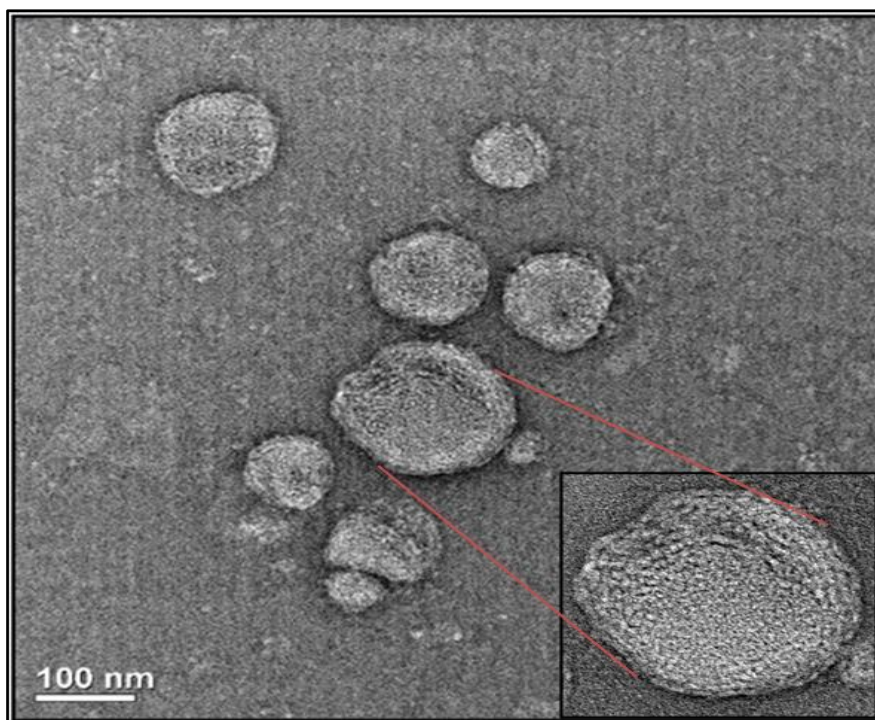


Figure – 6.15. TEM photograph of RSNa loaded glycosomes  
(Inset image shows single vesicle)

### 6.23.4. FTIR Study:

The FTIR spectra of RSNa and RSNa loaded glycosomes are shown in figure- 6.16. The RSNa spectra showed distinct peak in region of hydroxyl group which is associated with the O=P-OH of the phosphate group in the spectral region of 1585-1740  $\text{cm}^{-1}$  and found at 1652.5  $\text{cm}^{-1}$ . The characteristic peaks of phosphate group (P=O stretching) were observed within range of 910-1040  $\text{cm}^{-1}$  and found at 931.62  $\text{cm}^{-1}$ . The CO-H vibration corresponding to -OH groups was observed at 3363.56  $\text{cm}^{-1}$ . There was negligible change observed in the frequencies of characteristics peak of RSNa loaded in glycosomes. Hence, it was concluded that the RSNa was maintaining its structural integrity and compatibility with all excipients.

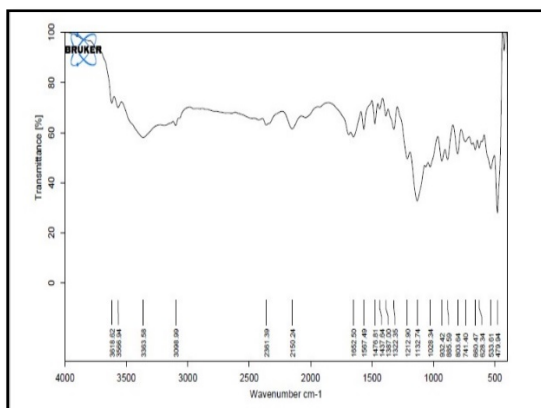


Figure- 6.16.A. FTIR spectra of RSNa

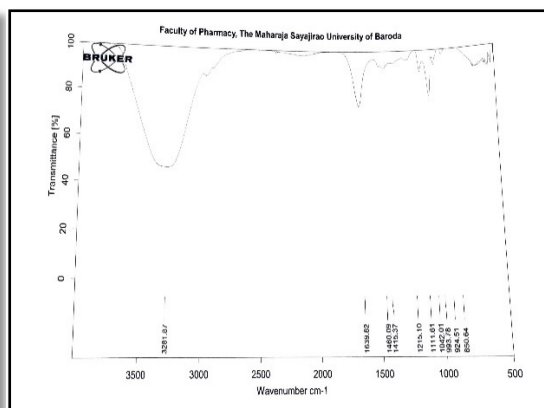


Figure- 6.16.B. FTIR spectra of RSNa loaded glycosomes

### 6.23.5. Residual solvent study:

The chromatogram of standard chloroform and methanol showed peak areas of 1437.47 and 1224.41 respectively. According to ICH guidelines Q3C for residual solvent, Chloroform, and methanol limits upto 600  $\mu\text{g/mL/day}$  and 3000  $\mu\text{g/mL/day}$  respectively is considered as safe. The residue of methanol was found to be 2.58  $\mu\text{g/mL}$ , while the residue of chloroform was found to be 20.94  $\mu\text{g/mL}$  in RSNa loaded glycosomes. It was concluded that chloroform and methanol are present much below their residual limits in the prepared formulations and considered safe for further use.

### 6.24. Optimization and impact of glycerol concentration on physicochemical characterization of RSNa loaded glycosomes:

The effects of glycerol concentration on physicochemical characteristics viz. average vesicles size, size distribution, surface charge, entrapment efficiency, deformability index was compared with liposomes (considered as 0% w/w glycerol containing glycosomes) as shown in table- 6.21.

Table-6.21. Physicochemical characterization of RSNa loaded glycosomes

<b>Glycosomes</b>						
<b>containing</b>	<b>Vesicle</b>		<b>Zeta</b>			
<b>glycerol</b>	<b>Size</b>	<b>PDI</b>	<b>Potential</b>	<b>% EE</b>	<b>% DLC</b>	<b>DI (%)</b>
<b>concentration</b>	<b>(d.nm)</b>		<b>(mV)</b>			
<b>(% w/w)</b>						
<b>0</b>	97.4 ±	0.375 ±	-10.2 ±	39.71 ±	2.00 ±	11.38 ±
<b>(RGLY<sub>0</sub>)</b>	3.39	0.071	1.27	0.92	0.092	0.892
<b>10</b>	143.5 ±	0.426 ±	-16.4 ±	48.98 ±	2.44 ±	25.17 ±
<b>(RGLY<sub>10</sub>)</b>	4.36	0.038	0.96	1.59	0.089	2.046
<b>20</b>	153.8 ±	0.213 ±	-18.3 ±	59.30 ±	2.99 ±	34.81 ±
<b>(RGLY<sub>20</sub>)</b>	6.90	0.035	1.00	1.08	0.055	2.501
<b>30</b>	170.2 ±	0.246 ±	-16.3 ±	65.06 ±	3.27 ±	39.95 ±
<b>(RGLY<sub>30</sub>)</b>	6.74	0.048	1.05	1.32	0.127	2.858

(n=3, ± S.D.)

\*PDI- Polydispersity Index, % EE- % Entrapment efficiency, % DLC- Drug loading capacity, DI- Deformability Index.

The results from table-6.21 revealed that increase in concentration of glycerol increases vesicles size as well as entrapment efficiency. The increase in vesicles size of formulations with an increase in the glycerol concentration might be due to sticky texture of glycerol [3, 28]. The Zeta potential of all formulations was found to be more than -10 mV. The zeta potential was not significantly affected by change in glycerol concentration. There was an increase in deformability index observed with an increase in glycerol concentration. The increasing order for DI was found to be RGLY<sub>0</sub> < RGLY<sub>10</sub> < RGLY<sub>20</sub> < RGLY<sub>30</sub>. From the results, it was concluded that glycerol acted as edge activator for lipid bilayer.

### 6.25. Rheological studies:

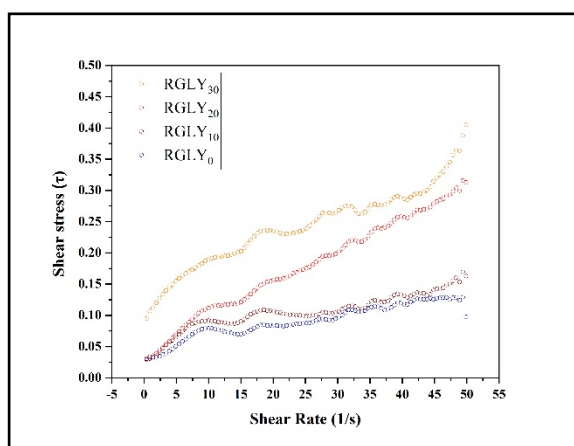
The results of rheological study are represented in figure- 6.17. Figure- 6.17.a represents graph of shear rate vs shear stress ( $\tau$ ) and figure- 6.17.b represents graph of shear rate vs viscosity ( $\eta$ ). Figure- 6.17.c represents graph of logarithmic form of shear rate and

viscosity ( $\eta$ ). Table- 6.22 summarized the values of  $\eta_0$ , K, and  $R^2$  (statistical correlation coefficient) produced from fitting of shear rate vs shear stress data.

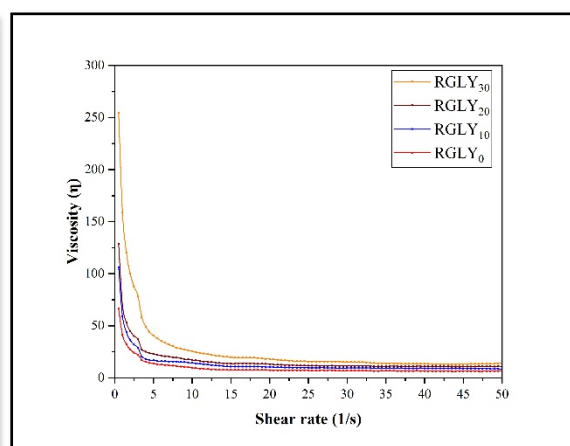
Figure 6.17a clearly showed that the shear stress increases as the shear rate increases linearly, implying newtonian behaviour of glycosomes. From the results (figure-6.17b), it was clearly observed that there was shear thinning or pseudoplastic behaviour of glycosomes. The zero-shear viscosity ( $\eta_0$ ) of RGLY<sub>0</sub>, RGLY<sub>10</sub>, RGLY<sub>20</sub> and RGLY<sub>30</sub> was found to be 100.34, 164.16, 203.70, and 368.56 mPas. The results of  $\eta_0$  revealed an increase in viscosity as a result of an increase in glycerol concentration. The apparent viscosity (K) was found to be 66.40, 100.26, 120.74, and 248.49 mPas for RGLY<sub>0</sub>, RGLY<sub>10</sub>, RGLY<sub>20</sub> and RGLY<sub>30</sub>. The flow behaviour index (n) is a measurement of a system's deviation from Newtonian behaviour. The "n" value was found to be 0.39, 0.35, 0.68, and 0.34 for RGLY<sub>0</sub>, RGLY<sub>10</sub>, RGLY<sub>20</sub> and RGLY<sub>30</sub>, implying shear thinning ( $n < 1$ ) behaviour of glycosomes, which is suitable for transdermal drug delivery [29-31].

Table- 6.22. Rheological power law fitting parameters for glycosomes

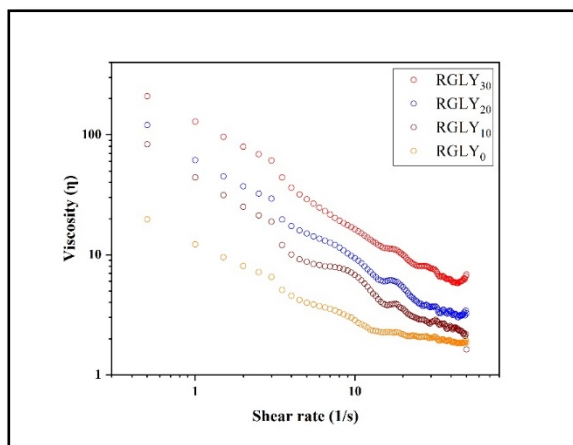
Formulations	$\eta_0$	K	n	$R^2$
RGLY <sub>0</sub>	100.34	66.40	0.39	0.9934
RGLY <sub>10</sub>	164.16	100.26	0.35	0.9033
RGLY <sub>20</sub>	203.70	120.74	0.68	0.9893
RGLY <sub>30</sub>	368.56	248.49	0.34	0.9261



a. Shear rate Vs shear stress ( $\tau$ )



b. Shear rate Vs Viscosity ( $\eta$ )



c. Logarithmic form of shear rate and viscosity ( $\eta$ )

Figure- 6.17. Different graph for rheological studies.

- a. Shear rate Vs shear stress ( $\tau$ )
- b. Shear rate Vs Viscosity ( $\eta$ )
- c. Logarithmic form of shear rate and viscosity ( $\eta$ )

#### 6.26. *In vitro* drug release study:

Figure- 6.18. represents drug release from RSNa solution and RSNa loaded glycrosomes to check effect of glycerol concentration on drug release in saline phosphate buffer pH 7.4 and pH 5.5. From the results (table-6.23), it was observed that 99.50 % of RSNa released from the RSNa solution within 3 hrs, while 84.05 %, 78.74 %, 72.22 %, 68.39 % of cumulative drug released from RGLY<sub>0</sub>, RGLY<sub>10</sub>, RGLY<sub>20</sub> and RGLY<sub>30</sub> within 48 hrs in PBS pH 5.5 which represents the pH of skin layers.

From the results (table-6.24), it was observed that 98.94 % of drug released from RSNa solution within 3 hrs, while 98.35 % of drug released from RGLY<sub>0</sub> within 36 hrs in PBS pH 7.4. While, 97.27 %, 95.53 % and 88.22 % drug released from RGLY<sub>10</sub>, RGLY<sub>20</sub> and RGLY<sub>30</sub> within 48 hrs respectively in PBS pH 7.4. These results revealed that as the amount of glycerol increased, drug release decreased, which was attributed to an increase in vesicle size with an increase in glycerol concentration, as previously mentioned, which decreased the available surface area for drug release [1, 32].

The data obtained from in-vitro drug release studies was fitted to the various release models like Zero-order, First order, Higuchi model and Korsmeyer-Peppas model. The regression-coefficient of the plot of zero order release kinetic model for RSNa solution

was found to be 0.9877, while regression-coefficient of the plot of first order release kinetic model for RGLY<sub>0</sub>, RGLY<sub>10</sub>, RGLY<sub>20</sub> and RGLY<sub>30</sub> was found to be 0.9900, 0.9912, 0.9758 and 0.9932 respectively in PBS pH 5.5. The release pattern followed anomalous transport release mechanism ( $n > 0.5$ ) for all glycosomes formulation and liposomes in PBS pH 5.5.

In case of PBS pH 7.4, the RSNa solution followed zero order kinetic model and regression-coefficient of the plot was found to be 0.9565, while RGLY<sub>0</sub>, RGLY<sub>10</sub>, and RGLY<sub>20</sub> followed first order release kinetic model and regression-coefficient of the plot was found to be 0.9545, 0.9910 and 0.9791 respectively. The RGLY<sub>30</sub> followed Higuchi model and regression-coefficient of the plot was found to be 0.9753. The release pattern followed anomalous transport release mechanism ( $n > 0.5$ ) for all glycosomes formulation and liposomes in PBS pH 7.4.

Table- 6.23. *In vitro* drug release profile for RSNa loaded glycosomes in pH 5.5

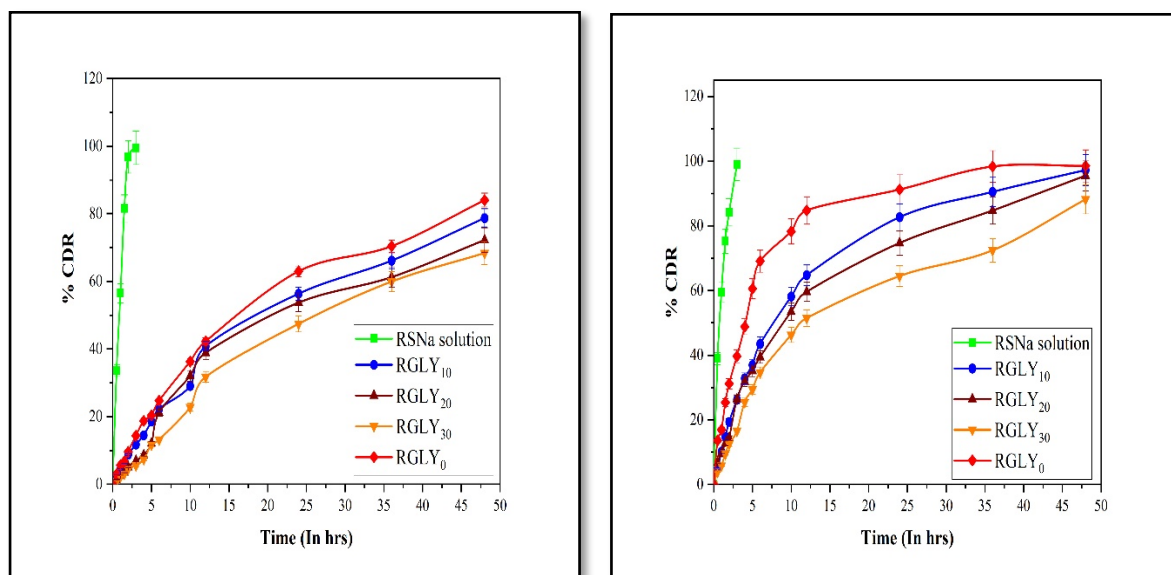
Time (In Hrs)	RSNa solution	RGLY <sub>0</sub>	RGLY <sub>10</sub>	RGLY <sub>20</sub>	RGLY <sub>30</sub>
0	0 ± 0	0 ± 0	0 ± 0	0 ± 0	0 ± 0
0.5	33.57 ± 3.26	2.99 ± 1.25	2.81 ± 0.98	1.41 ± 0.74	1.03 ± 0.61
1	56.50 ± 2.58	5.62 ± 2.51	4.41 ± 1.32	2.59 ± 0.96	2.25 ± 1.24
1.5	81.57 ± 4.96	6.76 ± 1.68	6.37 ± 1.22	3.58 ± 1.06	3.07 ± 1.03
2	96.83 ± 5.53	9.59 ± 1.96	8.75 ± 1.53	5.09 ± 2.51	4.55 ± 1.63
3	99.50 ± 3.32	14.36 ± 2.15	11.75 ± 1.85	6.96 ± 1.33	5.53 ± 1.37
4		18.73 ± 3.02	14.48 ± 1.62	8.60 ± 2.55	7.38 ± 1.21
5		20.36 ± 1.20	18.58 ± 2.21	12.13 ± 1.58	11.69 ± 1.63
6		24.71 ± 2.22	22.28 ± 2.02	21.17 ± 1.33	13.18 ± 1.02
10		36.31 ± 1.50	29.07 ± 1.54	32.04 ± 2.01	22.76 ± 1.84
12		42.27 ± 1.41	40.82 ± 1.78	38.88 ± 2.36	31.75 ± 0.98
24		63.00 ± 2.36	56.38 ± 1.65	53.73 ± 1.24	47.44 ± 0.66
36		70.43 ± 3.32	66.13 ± 2.64	61.27 ± 1.32	59.94 ± 1.25
48		84.05 ± 2.25	78.74 ± 1.96	72.22 ± 1.21	68.39 ± 1.78

(n=3, ±S.D.)

Table- 6.24. *In vitro* drug release profile of RSNa loaded glycosomes in pH 7.4

Time (In Hrs)	RSNa solution	RGLY <sub>0</sub>	RGLY <sub>10</sub>	RGLY <sub>20</sub>	RGLY <sub>30</sub>
0	0 ± 0	0 ± 0	0 ± 0	0 ± 0	0 ± 0
0.5	38.99 ± 4.32	13.67 ± 1.32	4.83 ± 0.84	6.76 ± 1.74	3.93 ± 1.38
1	59.51 ± 5.13	16.94 ± 1.28	10.10 ± 1.68	9.59 ± 1.00	5.88 ± 1.57
1.5	75.24 ± 4.52	25.38 ± 1.73	14.74 ± 1.32	12.70 ± 1.58	9.52 ± 1.28
2	84.19 ± 6.43	31.18 ± 2.14	19.39 ± 1.09	14.38 ± 2.03	12.53 ± 2.35
3	98.94 ± 2.02	39.69 ± 2.65	26.23 ± 1.84	26.37 ± 2.51	16.56 ± 3.63
4		48.82 ± 1.95	32.87 ± 2.62	31.88 ± 1.48	25.50 ± 1.58
5		60.58 ± 1.11	36.96 ± 1.61	35.17 ± 1.69	29.41 ± 2.14
6		69.12 ± 1.96	43.49 ± 1.24	39.45 ± 1.99	34.65 ± 1.75
10		78.29 ± 1.78	58.16 ± 1.87	53.47 ± 2.68	46.28 ± 1.98
12		84.79 ± 2.15	64.77 ± 2.64	59.59 ± 1.47	51.45 ± 1.24
24		91.27 ± 3.32	82.71 ± 2.98	74.71 ± 1.98	64.49 ± 1.26
36		98.35 ± 2.28	90.53 ± 2.84	84.74 ± 2.50	72.43 ± 2.74
48		98.56 ± 2.23	97.27 ± 2.14	95.53 ± 2.88	88.22 ± 2.63

(n=3, ±S.D.)



(a)

(b)

Figure-6.18. Comparison of % cumulative drug release of RSNa solution and RSNa loaded glycosomes containing different glycerol concentration (0-30% w/w) in (a) pH 5.5 and (b) pH 7.4.

Table- 6.25. Drug release kinetic models for RSNa loaded glycerosomes in pH 5.5

Kinetic Models	RSNa solution	RGLY <sub>0</sub>	RGLY <sub>10</sub>	RGLY <sub>20</sub>	RGLY <sub>30</sub>
Zero order	<b>0.9877</b>	0.9201	0.9378	0.9114	0.9576
First order	0.8440	<b>0.9900</b>	<b>0.9912</b>	<b>0.9758</b>	<b>0.9932</b>
Higuchi	0.9473	0.9874	0.9852	0.9662	0.9693
Korsemeyer-Peppas (n)	0.2372 (0.543)	0.8685 (0.600)	0.8694 (0.636)	0.9364 (0.673)	0.7868 (0.757)

Table- 6.26. Drug release kinetic models for RSNa loaded glycerosomes in pH 7.4

Kinetic Models	RSNa solution	RGLY <sub>0</sub>	RGLY <sub>10</sub>	RGLY <sub>20</sub>	RGLY <sub>30</sub>
Zero order	<b>0.9565</b>	0.6375	0.8219	0.8482	0.8672
First order	0.8909	<b>0.9554</b>	<b>0.9910</b>	<b>0.9791</b>	0.9681
Higuchi	0.9339	0.8556	0.9641	0.9741	<b>0.9753</b>
Korsemeyer-Peppas (n)	0.0970 (0.490)	0.5607 (0.474)	0.7454 (0.466)	0.7379 (0.479)	0.8143 (0.519)

### 6.27. *Ex vivo* skin permeation study:

The results of *ex-vivo* skin permeation study are shown in figure-6.19 and table-6.27. The % cumulative drug permeated through skin by RSNa solution was 20.93 %, while RSNa loaded liposomes permeated 37.45 % of RSNa through skin in 48 hrs. The amount of RSNa permeated through rat skin in RGLY<sub>0</sub>, RGLY<sub>10</sub>, RGLY<sub>20</sub> and RGLY<sub>30</sub> was 55.46 %, 59.97 % and 72.72 % respectively. The amount of RSNa permeated through skin was enhanced -2.40, -2.95 and -3.43 folds in comparison with RSNa solution; while -1.42, -1.67 and -2.01 folds enhanced for RGLY<sub>10</sub>, RGLY<sub>20</sub> and RGLY<sub>30</sub> respectively as compared with RGLY<sub>0</sub> respectively. Based on results (table-6.27), it was observed that the increase in concentration of glycerol in glycerosomes increased permeation of RSNa through skin. The RGLY<sub>30</sub> showed maximum drug permeation which might be due to the highly deformable nature of vesicles [33].

The average flux (amount of drug permeated per area per time;  $\mu\text{g}/\text{cm}^2/\text{hr}$ ) of RSNa solution was found to be 1.94  $\mu\text{g}/\text{cm}^2/\text{hr}$  while average flux for RGLY<sub>0</sub>, RGLY<sub>10</sub>, RGLY<sub>20</sub> and RGLY<sub>30</sub> was found to be 3.26, 4.65, 5.44, and 6.57  $\mu\text{g}/\text{cm}^2/\text{hr}$  respectively

and it was higher as compared to RSNa solution and RGLY<sub>0</sub>. The steady state flux of RSNa solution and RGLY<sub>0</sub> was found to be 1.65 and 3.02  $\mu\text{g}/\text{cm}^2/\text{hr}$ , while steady state flux for RGLY<sub>10</sub>, RGLY<sub>20</sub> and RGLY<sub>30</sub> was found to be 4.39, 4.86 and 5.66  $\mu\text{g}/\text{cm}^2/\text{hr}$ . Based on the results, it was found that an increase in the concentration of glycerol enhanced transdermal flux. The ability of glycerol to alter the stratum corneum lipid structure and to increase the flexibility and hydration of stratum corneum may be the reason for the enhanced flux rate of glycosomes [34]. The characteristics of elastic and deformable nature appear to be combined in these novel RSNa loaded glycosomes. These properties of glycerol help to decrease the skin's natural barrier, which enhances the penetration of vesicles through the skin [34].

Table- 6.27. *Ex vivo* skin permeation profile of RSNa loaded glycosomes

Time (In hrs)	RGLY <sub>30</sub>	RGLY <sub>20</sub>	RGLY <sub>10</sub>	RGLY <sub>0</sub>	RSNa solution
0	0 ± 0	0 ± 0	0 ± 0	0 ± 0	0 ± 0
1	0.88 ± 0.25	0.75 ± 0.36	0.45 ± 0.31	0.13 ± 0.09	0 ± 0
2	1.93 ± 0.74	1.62 ± 0.53	1.85 ± 0.87	1.55 ± 0.68	0.09 ± 0.04
3	3.55 ± 1.32	3.21 ± 1.41	2.95 ± 1.19	2.05 ± 1.04	0.56 ± 0.25
4	6.10 ± 1.62	4.55 ± 1.99	4.56 ± 2.31	2.70 ± 1.24	1.21 ± 0.63
5	9.33 ± 1.24	7.22 ± 2.18	7.73 ± 1.31	4.19 ± 2.40	2.90 ± 1.02
6	15.33 ± 1.69	12.08 ± 2.61	11.01 ± 1.77	6.05 ± 1.84	2.58 ± 0.87
8	22.46 ± 2.51	17.21 ± 1.84	13.00 ± 1.45	9.16 ± 2.14	3.27 ± 1.26
10	26.16 ± 3.62	23.09 ± 2.69	16.25 ± 2.54	13.52 ± 2.63	5.20 ± 0.98
12	32.46 ± 2.15	26.57 ± 1.52	21.47 ± 2.65	18.83 ± 1.05	7.26 ± 1.58
24	44.15 ± 3.65	39.15 ± 1.89	35.82 ± 1.99	23.27 ± 1.97	9.10 ± 1.36
30	53.20 ± 2.84	47.45 ± 3.11	43.28 ± 1.47	29.15 ± 1.84	15.25 ± 2.01
36	61.20 ± 2.81	52.84 ± 2.47	48.39 ± 2.14	31.69 ± 1.56	16.32 ± 2.24
48	72.72 ± 5.21	59.97 ± 2.95	55.46 ± 3.02	37.45 ± 1.73	20.93 ± 1.52

Parameters	RGLY <sub>30</sub>	RGLY <sub>20</sub>	RGLY <sub>10</sub>	RGLY <sub>0</sub>	Pure RSNa
<b>Drug remained on skin (%)</b>	9.53 ± 2.25	18.43 ± 1.83	29.90 ± 2.04	32.84 ± 2.21	68.22 ± 4.54
<b>Drug retained in the skin (%)</b>	16.10 ± 2.52	13.90 ± 2.54	13.77 ± 1.94	26.74 ± 1.79	10.96 ± 1.79
<b>Transdermal flux (µg/cm<sup>2</sup>/hr)</b>	6.57	5.44	4.65	3.26	1.94
<b>Steady state flux</b>	5.66	4.86	4.39	3.02	1.65
<b>PER (as compared to pure drug)</b>	3.43	2.95	2.40	1.98	1
<b>PER (as compared to RGLY<sub>0</sub>)</b>	2.01	1.67	1.42	1	-

(n=3, ±S.D.)

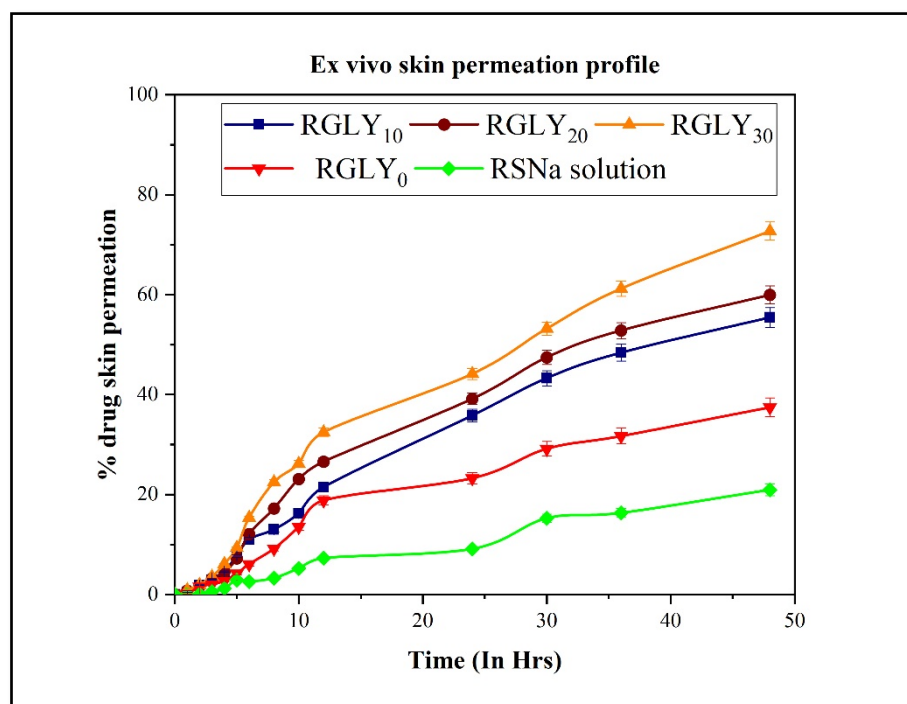


Figure- 6.19. Ex vivo skin permeation profile of RSNa loaded glycosomes

The RSNa solution showed the maximum amount of drug remaining and the minimum amount of drug retained in the skin. This might be due to the highly polar and hydrophilic nature of RSNa, whose penetration is restricted by the lipid layers of the stratum corneum [31]. All glycosomal formulations showed minimum drug remained on skin as compared to RSNa solution and liposomes due to the elastic nature of glycosomes which easily squeezed through membrane pores and permeated through skin.

#### **6.28. Optimization of glycerol concentration in RSNa loaded glycosomes:**

On the basis of results of physicochemical characteristics, *in vitro* drug release and *ex vivo* skin permeation studies of 10 to 30% w/w glycerol containing RSNa loaded glycosomes, it was revealed that the 30% w/w glycerol containing RSNa loaded glycosomes (RGLY<sub>30</sub>) showed better skin penetration and permeation (shown in figure-6.19 and table- 6.27), sustained drug release (shown in table- 6.23 & 6.24 and figure- 6.18), better entrapment efficiency, drug loading capacity, and higher deformability index of glycosomes (shown in table- 6.21). Based on above experimental results, 30 % w/w glycerol containing RSNa loaded glycosomes (RGLY<sub>30</sub>) was optimized and chosen for further *ex vivo* studies, *in vitro* cell line studies and *in vivo* pharmacokinetic and pharmacodynamic studies.

#### **6.29. *In vitro* cell viability study:**

The results of the cell viability study, as shown in figure- 6.20, showed that the RSNa loaded glycosomes and placebo glycosomes were more viable for fibroblast cells for 24 hrs. The RSNa loaded liposomes and placebo liposomes also showed better viability and no remarkable difference as compared to glycosomes. The RSNa solution showed slightly less viability as compared to placebo and drug loaded formulations. There was no remarkable difference observed with change in concentration of RSNa loaded formulations. From the results, it was revealed that the RSNa loaded glycosomes will be safe and non-toxic vesicular nanocarrier for transdermal drug delivery.

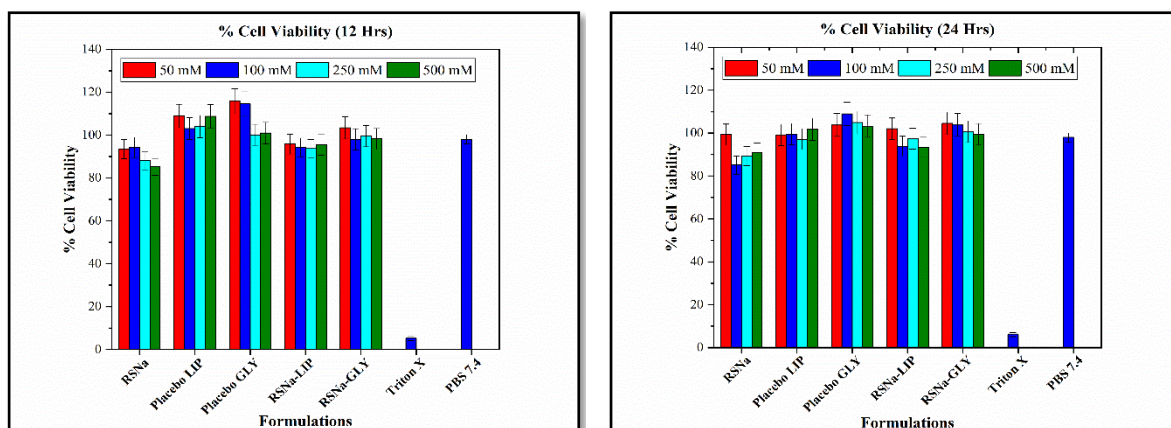


Figure- 6.20. % cell viability study (a) 12 hrs and (b) 24 hrs.

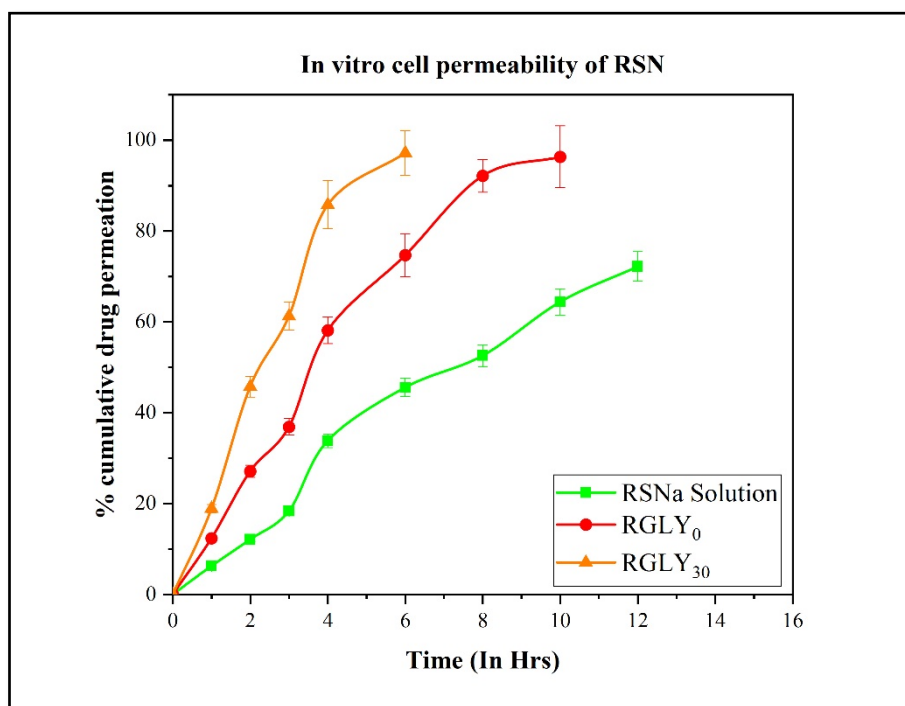
### 6.30. *In vitro* cell permeability study:

Transepithelial/transendothelial electrical resistance (TEER) value for cell permeability was found in the range of 920-950  $\Omega\text{cm}^2$  (accepted limit is 500-1100  $\Omega\text{cm}^2$ ) and it showed good quality of monolayer development on the basement [35-37]. The results of the cell permeability study are shown in table- 6.28 and figure- 6.21. The RGLY<sub>30</sub> and RGLY<sub>0</sub> exhibited  $P_{\text{app}}$  value of  $1.63 \times 10^{-5}$  cm/s and  $1.04 \times 10^{-5}$  cm/s respectively. While RSNa solution exhibited the  $P_{\text{app}}$  value of  $5.53 \times 10^{-6}$  cm/s. The results showed significant difference ( $p < 0.05$ ) in permeation of drug through cell layer for RSNa solution, RGLY<sub>0</sub> and RGLY<sub>30</sub>. The RSNa loaded glycosomes were more permeable as compared to the RGLY<sub>0</sub> and RSNa solution through the fibroblast cell layer. The possible reason behind more permeability was the presence of glycerol in the formulation, which makes vesicles elastic, and nanosized structures, which facilitate the permeation of vesicles through cell layers.

Table- 6.28. *In vitro* cell permeability profile

Time (In Hrs)	RSNa solution	RGLY <sub>0</sub>	RGLY <sub>30</sub>
0	0 ± 0	0 ± 0	0 ± 0
1	6.27 ± 2.36	12.36 ± 4.88	18.88 ± 2.15
2	12.12 ± 3.94	27.12 ± 3.47	45.75 ± 4.21
3	18.35 ± 4.76	36.88 ± 5.21	61.26 ± 5.69
4	33.88 ± 4.18	58.15 ± 5.55	85.78 ± 7.14
6	45.56 ± 3.44	74.69 ± 6.26	97.20 ± 4.61
8	52.57 ± 5.94	92.15 ± 4.78	
10	64.40 ± 3.74	96.33 ± 5.11	
12	72.19 ± 3.87		
$P_{app}$ (cm/s)	$5.53 \times 10^{-6}$	$1.04 \times 10^{-5}$	$1.63 \times 10^{-5}$

(n=3, ±S.D.)

Figure- 6.21. *In vitro* cell permeability profile

### 6.31. Stability study:

The effect of storage conditions on physicochemical parameters like vesicle size and % assay is shown in table- 6.29 and figure- 6.22. There was no significant change in vesicle size and % assay of glycosomes formulation on storage at 2-8°C (A and D) and 25±2°C/60±5 % RH (B and E). There was slight increase in vesicle size and slight decrease in % assay at 40±2°C/75±5% RH (C and F) due to the viscous nature of glycosomal dispersion, lowering the possibility of agglomeration [4, 25]. While, in case of 0% glycosomes (liposomes), the average vesicle size was increased and % assay was decreased at 25±2°C/60±5 % RH as well as 40°C/75±5 % RH. As previously observed, glycerol appeared to stabilise the vesicle dispersion, avoiding aggregation or fusion, which was not there in liposome [38]. On the basis of results, it was revealed that RSNa loaded glycosomes were stable at 2-8°C and 25±2°C/60±5 % RH for more than 90 days as compared to RSNa loaded liposomes.

Table- 6.29. Stability study profile at different storage condition

Sr. No.	Time interval (In Month)	Formulations	Vesicle Size (d.nm)			% Assay		
			2-8°C	25±2°C/60±5 % RH	40±2°C/75±5 % RH	2-8°C	25±2°C/60±5 % RH	40±2°C/75±5 % RH
1	Initial	RGLY <sub>0</sub>	97.4 ± 3.39	97.4 ± 3.39	97.4 ± 3.39	99.15 ± 1.95	99.15 ± 1.95	99.15 ± 1.95
		RGLY <sub>30</sub>	170.6 ± 6.74	170.6 ± 6.74	170.6 ± 6.74	98.80 ± 1.04	98.80 ± 1.04	98.80 ± 1.04
2	0.5	RGLY <sub>0</sub>	99.3 ± 4.96	101.6 ± 4.87	128.4 ± 6.42	98.27 ± 0.91	97.26 ± 1.28	96.25 ± 1.12
		RGLY <sub>30</sub>	166.6 ± 5.97	178.3 ± 8.90	189.3 ± 4.94	98.07 ± 0.87	97.86 ± 0.84	98.03 ± 1.36
3	1.0	RGLY <sub>0</sub>	100.8 ± 6.04	109.9 ± 7.08	138.2 ± 6.91	98.60 ± 0.73	96.21 ± 0.68	95.63 ± 1.07
		RGLY <sub>30</sub>	174.3 ± 5.83	175.8 ± 4.76	194.7 ± 4.73	98.65 ± 0.63	98.18 ± 0.39	96.18 ± 2.69
4	1.5	RGLY <sub>0</sub>	108.3 ± 5.42	105.7 ± 6.49	146.5 ± 7.32	96.21 ± 1.81	94.15 ± 0.97	96.24 ± 1.08
		RGLY <sub>30</sub>	172.8 ± 6.10	168.2 ± 8.44	185.6 ± 5.28	98.78 ± 1.23	97.26 ± 1.36	97.14 ± 1.11
5	2.0	RGLY <sub>0</sub>	105.1 ± 7.25	128.5 ± 8.38	176.8 ± 8.84	97.68 ± 0.88	95.84 ± 1.58	93.04 ± 0.98
		RGLY <sub>30</sub>	175.5 ± 7.04	172.1 ± 6.61	193.7 ± 6.68	99.88 ± 0.49	96.85 ± 1.36	94.84 ± 1.84
6	2.5	RGLY <sub>0</sub>	107.6 ± 4.38	121.8 ± 6.42	210.8 ± 12.54	97.42 ± 1.37	93.14 ± 1.47	95.74 ± 2.21
		RGLY <sub>30</sub>	172.1 ± 7.13	179.6 ± 5.98	200.8 ± 8.01	97.86 ± 1.43	97.74 ± 0.93	92.18 ± 2.88
7	3.0	RGLY <sub>0</sub>	116.3 ± 5.81	142.3 ± 7.11	200.2 ± 10.01	96.84 ± 0.94	94.58 ± 2.21	90.30 ± 1.22
		RGLY <sub>30</sub>	180.3 ± 6.02	185.4 ± 6.27	208.6 ± 10.43	98.32 ± 1.16	98.05 ± 1.35	93.66 ± 1.33

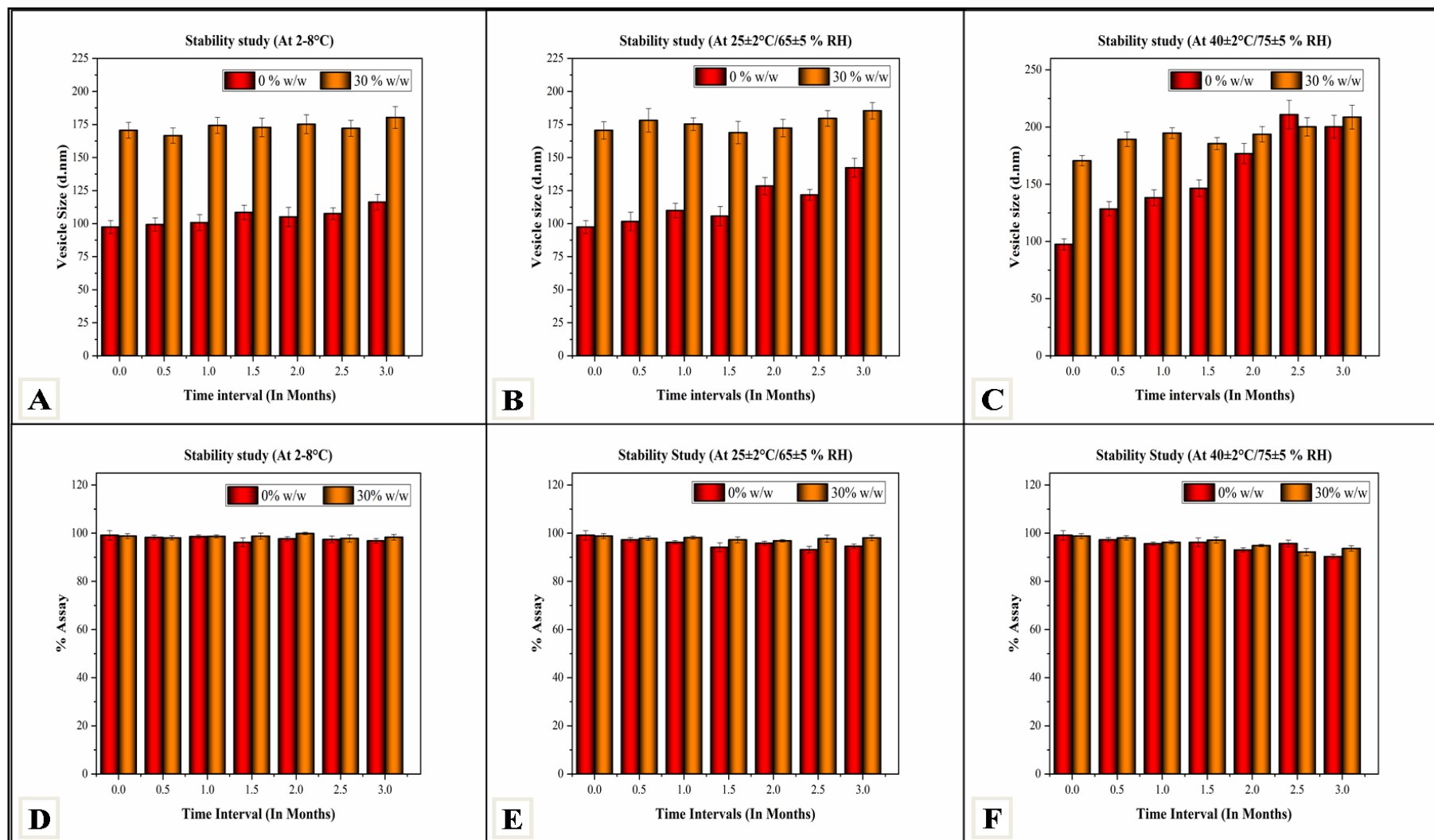


Figure- 6.22. Stability study profile of RSNa loaded liposomes (0% w/w glycerol containing) and RSNa loaded glycosomes at 2-8°C (A and D), 25±2°C/65±5 % RH (B and E), 40±2°C/75±5 % RH (C and F).

## Chapter 6 – RSNa loaded Glycosomes

### 6.32. References:

1. Salem, H.F., et al., *Formulation design and optimization of novel soft glycosomes for enhanced topical delivery of celecoxib and cupferron by Box–Behnken statistical design*. Drug Development and Industrial Pharmacy, 2018. **44**(11): p. 1871-1884.
2. Manca, M.L., et al., *Glycosomes: A new tool for effective dermal and transdermal drug delivery*. International Journal of Pharmaceutics, 2013. **455**(1-2): p. 66-74.
3. Zhang, K., et al., *Essential oil-mediated glycosomes increase transdermal paeoniflorin delivery: Optimization, characterization, and evaluation In vitro and in vivo*. International journal of nanomedicine, 2017. **12**: p. 3521.
4. Manca, M.L., et al., *Glycosomes: Use of hydrogenated soy phosphatidylcholine mixture and its effect on vesicle features and diclofenac skin penetration*. International Journal of Pharmaceutics, 2016. **511**(1): p. 198-204.
5. Rani, D., et al., *Formulation development and in-vitro evaluation of minoxidil bearing glycosomes*. Am. J. Biomed. Res, 2016. **4**: p. 27-37.
6. Han, E.-J., A.-H. Chung, and I.-J. Oh, *Analysis of residual solvents in poly (lactide-co-glycolide) nanoparticles*. Journal of Pharmaceutical Investigation, 2012. **42**(5): p. 251-256.
7. Yang, Y., X.Y. Xie, and X.G. Mei, *Preparation and In vitro evaluation of thienorphine-loaded PLGA nanoparticles*. Drug delivery, 2016. **23**(3): p. 777-783.
8. Grodowska, K. and A. Parczewski, *Analytical methods for residual solvents determination in pharmaceutical products*. Acta Poloniae Pharmaceutica. Drug Research, 2010. **67**(1).
9. Zhang, K., et al., *Preparation, characterization, and in vivo pharmacokinetics of nanostructured lipid carriers loaded with oleanolic acid and gentiopicrin*. International journal of nanomedicine, 2013. **8**: p. 3227.
10. Duangjit, S., et al., *Characterization and In vitro skin permeation of meloxicam-loaded liposomes versus transfersomes*. Journal of drug delivery, 2011. **2011**.

11. Dissette, V., et al., *Particulate adducts based on sodium risedronate and titanium dioxide for the bioavailability enhancement of oral administered bisphosphonates*. European journal of pharmaceutical sciences, 2010. **41**(2): p. 328-336.
12. Wavikar, P. and P.J.A.p. Vavia, *Nanolipidgel for enhanced skin deposition and improved antifungal activity*. AAPS PharmSciTech, 2013. **14**: p. 222-233.
13. Kim, H., et al., *Characteristics of skin deposition of itraconazole solubilized in cream formulation*. Pharmaceutics, 2019. **11**(4): p. 195.
14. Elshall, A.A., et al., *Ex vivo permeation parameters and skin deposition of melatonin-loaded microemulsion for treatment of alopecia*. Future Journal of Pharmaceutical Sciences volume, 2022. **8**(1): p. 28.
15. Chen, M., X. Liu, and A.J.I.j.o.p. Fahr, *Skin penetration and deposition of carboxyfluorescein and temoporfin from different lipid vesicular systems: In vitro study with finite and infinite dosage application*. International Journal of Pharmaceutics, 2011. **408**(1-2): p. 223-234.
16. Aboud, H.M., et al., *Development, optimization, and evaluation of carvedilol-loaded solid lipid nanoparticles for intranasal drug delivery*. AAPS pharmscitech, 2016. **17**(6): p. 1353-1365.
17. Segeritz, C.-P. and L. Vallier, *Cell culture: Growing cells as model systems In vitro*, in *Basic science methods for clinical researchers*. 2017, Elsevier. p. 151-172.
18. Helgason, C.D. and C.L. Miller, *Basic cell culture protocols*. 2005: Totowa, NJ.: Humana Press.
19. Tripathi, B.D. and N. Singh, *Wound Healing Potential of Transdermal Patches Containing Bioactive Fraction: A Novel Approach*. International Journal of Pharmacy & Life Sciences, 2020. **11**(7): p. 83-83.
20. Manca, M.L., et al., *Glycosomes: investigation of role of 1, 2-dimyristoyl-sn-glycero-3-phosphatidylcholine (DMPC) on the assembling and skin delivery performances*. International journal of pharmaceutics, 2017. **532**(1): p. 401-407.
21. Moolakkadath, T., et al., *Preparation and optimization of fisetin loaded glycerol based soft nanovesicles by Box-Behnken design*. International Journal of Pharmaceutics, 2020. **578**: p. 119125.

22. Naguib, M.J., et al., *Investigating the potential of utilizing glycosomes as a novel vesicular platform for enhancing intranasal delivery of lacidipine*. International Journal of Pharmaceutics, 2020. **582**: p. 119302.
23. He, Y., et al., *Influence of probe-sonication process on drug entrapment efficiency of liposomes loaded with a hydrophobic drug*. International Journal of Polymeric Materials and Polymeric Biomaterials, 2019. **68**(4): p. 193-197.
24. Yamaguchi, T., et al., *Effects of frequency and power of ultrasound on the size reduction of liposome*. Chemistry and Physics of Lipids, 2009. **160**(1): p. 58-62.
25. Naguib, M.J., Y.R. Hassan, and W.H.J.I.J.o.P. Abd-Elsalam, *3D printed ocusert laden with ultra-fluidic glycosomes of ganciclovir for the management of ocular cytomegalovirus retinitis*. International Journal of Pharmaceutics, 2021. **607**: p. 121010.
26. Rushmi, Z.T., et al., *The impact of formulation attributes and process parameters on black seed oil loaded liposomes and their performance in animal models of analgesia*. 2017. **25**(3): p. 404-412.
27. Sinico, C., et al., *Liposomes as carriers for dermal delivery of tretinoin: In vitro evaluation of drug permeation and vesicle–skin interaction*. Journal of Controlled Release, 2005. **103**(1): p. 123-136.
28. Moolakkadath, T., et al., *Preparation and optimization of fisetin loaded glycerol based soft nanovesicles by Box-Behnken design*. International journal of pharmaceutics, 2020. **578**: p. 119125.
29. Gupta, V., P.J.J.o.d.d.s. Trivedi, and technology, *Enhancement of storage stability of cisplatin-loaded protransfersome topical drug delivery system by surface modification with block copolymer and gelling agent*. Journal of Drug Delivery Science and Technology, 2012. **22**(4): p. 361-366.
30. Jain, A.K., et al., *Adapalene loaded solid lipid nanoparticles gel: an effective approach for acne treatment*. Colloids and Surfaces B: Biointerfaces, 2014. **121**: p. 222-229.
31. Gyanewali, S., et al., *Formulation development and In vitro–in vivo assessment of protransfersomal gel of anti-resorptive drug in osteoporosis treatment*. International Journal of Pharmaceutics, 2021. **608**: p. 121060.

32. Manca, M.L., et al., *Improvement of quercetin protective effect against oxidative stress skin damages by incorporation in nanovesicles*. Colloids and surfaces B: Biointerfaces, 2014. **123**: p. 566-574.
33. Manca, M.L., et al., *Close-packed vesicles for diclofenac skin delivery and fibroblast targeting*. Colloids and Surfaces B: Biointerfaces, 2013. **111**: p. 609-617.
34. Moolakkadath, T., et al., *Preparation and optimization of fisetin loaded glycerol based soft nanovesicles by Box-Behnken design*. 2020. **578**: p. 119125.
35. Shah, P., et al., *In vitro assessment of acyclovir permeation across cell monolayers in the presence of absorption enhancers*. Drug development and industrial pharmacy, 2008. **34**(3): p. 279-288.
36. Chen, S., R. Einspanier, and J. Schoen, *Transepithelial electrical resistance (TEER): a functional parameter to monitor the quality of oviduct epithelial cells cultured on filter supports*. Histochemistry and cell biology, 2015. **144**(5): p. 509-515.
37. Poenar, D.P., et al., *Low-cost method and biochip for measuring the trans-epithelial electrical resistance (TEER) of esophageal epithelium*. Materials, 2020. **13**(10): p. 2354.
38. Manca, M.L., et al., *Glycosomes: Investigation of role of 1, 2-dimyristoyl-sn-glycero-3-phosphatidylcholine (DMPC) on the assembling and skin delivery performances*. International Journal of Pharmaceutics, 2017. **532**(1): p. 401-407.